Ricardo César Silva Rêgo

Search for new physics at the Compact Linear Collider

Natal – RN

2024

Ricardo César Silva Rêgo

Search for new physics at the Compact Linear Collider

Master Thesis presented to the Graduate Program in Physics of the Federal University of Rio Grande do Norte as a partial requirement to obtain the degree of Master of Physics.

Federal University of Rio Grande do Norte

Graduate Program in Physics

Supervisor Prof. Dr. Farinaldo Queiroz

Co-supervisor: Dr. Yohan Mauricio Torres

Natal – RN

2024

Para a minha avó M. Lucia, obrigado por tudo...

Acknowledgements

Eu gostaria de agradecer primeiramente a minha mãe Lanna e meu pai Luciano por tudo, principalmente pelo suporte que me deram nestes últimos meses, além disso gostaria de agradecer a toda minha família: avós, tias, primos e primas que foram sempre muito compreensíveis e encorajadores com relação a minha carreira e ambições. Gostaria de agradecer ao meu namorado Wesley por ficar comigo e me apoiar nessa fase da minha vida, bem como pela ajuda em partes dessa dissertação. Também recebi ajuda de muitos amigos, portanto obrigado aos meus amigos Zé e Letícia pelas nossas frutíferas discussões e pelos dipironas, agradeço também a minha amiga Lucia e meu amigo Vítor pelas excelentes referências bibliográficas e discussões sobre a física, além disso também quero agradecer profundamente ao Dr. Maurício por me ajudar tanto a aprender sobre simulações e física de colisores. Gostaria também de agradecer ao meu orientador o Prof. Farinaldo, por me apoiar e guiar minhas decisões acadêmicas, bem como me ajudar no dia-a-dia a aprender sempre mais sobre a física.

Além disso também agradeço a CAPES pelo suporte financeiro. Por fim quero expressar meu profundo agradecimento a todos que me ajudaram, apoiaram e tornaram essa dissertação possível, muito obrigado.

"A new scientific truth does not triumph by convincing its opponents and making them see the light, but rather because its opponents eventually die, and a new generation grows up that is familiar with it."

Max Planck

Abstract

Neste trabalho primeiramente revisamos os aspectos fundamentais do Modelo Padrão das interações eletrofracas, abordando bases teóricas como a importância das simetrias de gauge e da quebra espontânea de simetria para a geração de massas de partículas e o surgimento das interações entre férmions e bósons de gauge. Posteriormente, avançamos para Física Além do Modelo Padrão no âmbito de física de colisores motivados pelos futuros colisores planejados, em particular o Colisor Linear Compacto (CLIC). Nosso objetivo é estimar a capacidade do CLIC de descobrir um novo bóson vetorial massivo, um Z' leptofílico. Para isso, realizamos simulações de colisões elétron-pósitron no CLIC para o sinal e background em função de algumas variáveis cinemáticas e implementamos cortes que potencializem a razão signal-background. Com isso, concluímos que o CLIC tem um alto potencial de descobrir um Z' leptofílico com massas de até 3 TeV com menos de $10 fb^{-1}$ de luminosidade integrada, e um Z' de 5 TeV com uma luminosidade integrada de $1000 fb^{-1}$. Nosso trabalho destaca a capacidade do CLIC de alcançar sensibilidades significativas na detecção de um bóson vetorial Z' e estabelecer a existência de uma nova força fundamental na natureza.

Keywords: Standard Model; leptophilic Z' boson; collider physics; CLIC.

Abstract

In this work, we first review the fundamental aspects of the Standard Model of electroweak interactions, addressing theoretical foundations such as the importance of gauge symmetries and spontaneous symmetry breaking in the generation of particle masses and the emergence of interactions between fermions and gauge bosons. We then advance to Physics Beyond the Standard Model within the scope of collider physics, motivated by future planned colliders, particularly the Compact Linear Collider (CLIC). Our objective is to estimate the CLIC's capability to discover a new massive vector boson, a leptophilic Z'. To this end, we perform simulations of electron-positron collisions at the CLIC for both signal and background events as functions of certain kinematic variables and implement cuts that enhance the signal-to-background ratio. From this, we conclude that the CLIC has a high potential to discover a leptophilic Z' with masses up to 3 TeV with less than $10 fb^{-1}$ of integrated luminosity, and a Z' with a mass of 5 TeV with an integrated luminosity of $1000 fb^{-1}$. Our work underscores the CLIC's capability to achieve significant sensitivities in the detection of a Z' vector boson and to establish the existence of a new fundamental force in nature.

Keywords: Standard Model; leptophilic Z' boson; collider physics; CLIC.

List of Figures

List of Tables

Contents

Introduction

Over the last century, the Standard Model (MP) of particle physics has established itself as the most successful theoretical framework for describing elementary particles and the fundamental interactions that govern the universe. With an impressive level of predictive and experimental accuracy, the MP has been extensively tested on numerous processes involving elementary particles, from electromagnetic interaction to the weak and strong nuclear forces, including confirming notable predictions, such as the discovery of the Higgs boson. However, despite its extraordinary success, the MP has important gaps that indicate the need for a more comprehensive theory. Among these shortcomings are the inability to explain the nature of dark matter, the existence of which is widely supported by astrophysical observations but which has not yet been directly detected; the lack of a mechanism that explains the mass generation of neutrinos, which oscillates between different flavors, a phenomenon observed but not explained by the model; and the absence of a description for gravity, one of the fundamental forces of the universe, which remains disconnected from the theoretical framework of the MP. These challenges have motivated the search for new theories, in addition to MP, that can incorporate these gaps and offer a more complete understanding of natural phenomena, driving the advancement of particle physics beyond established boundaries.

The path to meeting these challenges has led to the development of theories that go beyond the limits of the Standard Model. These theories, often called "Beyond the Standard Model"(BSM), propose new particles, interactions, and symmetries that could potentially fill existing gaps and provide a more complete understanding of the fundamental forces that govern the universe. These new theoretical frameworks often consist of extensions, simple or complex, of the Standard Model symmetry group, and they hold the promise of addressing some of the most pressing questions in particle physics.

At the heart of exploring particle physics beyond the Standard Model (BSM) is the use of high-energy particle colliders. These devices play a key role in advancing our understanding of the subatomic world, allowing scientists to recreate extreme conditions that existed at the beginning of the universe, just moments after the Big Bang. State-of-the-art machines, such as the Large Hadron Collider (LHC) at CERN, have the ability to accelerate particles to speeds close to that of light and collide them with unprecedented energies. Through these collisions, we can investigate the fundamental building blocks of matter at scales never before achieved, opening up the possibility of revealing new particles or interactions predicted by BSM theories. To date, colliders such as the LHC have not found evidence of new physics, which has served as motivation for planning upgrades to the LHC or building future colliders such as the High Luminosity LHC (HL-LHC), the High Energy LHC (HE-LHC), the Future Circular Collider (FCC) and the Compact Linear Collider (CLIC). Due to the need for physics models BSM and

the fundamental role that particle colliders have for the exploration of this new physics, in this thesis we will deepen the study of a new Z' vector boson that arises from the Z' leptophilic model.

This work aims to be a study based on the paper "Searching for a Leptophilic Z' and a 3-3-1 Symmetry at CLIC"[1], which was chosen for its general approach in utilizing various concepts of collider physics, serving as a solid foundation for my introduction to the topic. Throughout the study, I became familiar with several packages used in collider event simulations, such as MADGRAPH, FEYNRULES, and CALCHEP, as well as the initial use of PYTHIA and DELPHES. I learned how to implement a beyond the Standard Model (BSM) model into the simulator, generate collision events in a detector, and process the data to extract kinematic variables and use them to identify Z' boson signals in the processes.

In the first chapter we will discuss in detail the Standard Model of electroweak interactions, its theoretical bases and the importance of gauge symmetries and spontaneous symmetry breaking for the generation of particle masses. We will explore how scalar, vector, and fermionic fields interact within this framework, as well as highlighting the crucial role played by the Higgs mechanism in unifying electromagnetic and weak interactions. In the second chapter we will delve into the study of collider physics, where we will address the interactions between high-energy particles, highlighting the relevant parameters of the colliders, the kinematic variables and the characteristics of the detectors used in the experimental analysis of these collisions. This is one of the fundamental pillars in researching new physics beyond the Standard Model. The third chapter will present a sensitivity study for detecting a new Z' boson at CLIC, where we will examine the experiment's potential to observe this new boson within the leptophilic Z' model. Finally, a conclusion will be provided, along with future perspectives.

1 Standard Model of electroweak interactions

The Standard Model (SM) of particle physics is one of the most well-tested models of recent decades, and its theoretical predictions were able to anticipate, for example, the existence of particles such as the top quark (1995), the tau neutrino (2000), and the Higgs boson (2012), long before they were observed. Predictions of new particles and their properties, as well as the description of their fundamental interactions have been confirmed with a high degree of precision. Despite its many achievements, it's widely acknowledged in the scientific community that the SM is incomplete. One of the open questions is that although it can describe weak, strong and electromagnetic interactions well, it does not describe gravitational interactions. In addition, there are several other problems in particle physics such as the existence of dark matter, the generation of neutrinos masses and oscillations, the anomalous magnetic moment of the muon (g-2), among others, which are not described by the SM.

From a historical perspective, the construction of the SM demanded extensive theoretical and experimental development throughout the 20th century. One of the processes that was highly relevant in the conception of the electroweak theory, and thus the SM, was the beta decay, which exhibited a continuous spectrum in the electron lines [2]. This is significant because it was expected that the decay would only proceed as $n \rightarrow p + e^-$, leading to a discrete electron spectrum. However, since this is not the case, it suggests the existence of a third particle causing the possible energies of the electron to vary continuously. This culminated in the hypothesis proposed by W. Pauli, suggesting the existence of a light, neutral, and weakly interacting particle generated in this decay [3], which would later be known as the neutrino, so that the beta decay process becomes $n \rightarrow p + e^- + \bar{\nu}$.

To explain the beta decay, E. Fermi proposed an effective field theory considering a point-like interaction between four fermions [4]. This kind of theory is an approximation, in the case of the four-Fermi theory it only works on low energy scales. Fermi drew inspiration from quantum electrodynamics (QED), one of the most successful theories in physics, so that the weak interaction of the beta decay could be described by a current-current type Lagrangian (1.1). However, the four-fermion theory proved to be incomplete, as its cross-section violates unitarity for P_{cm} greater than 300 GeV. To alleviate this problem, Schwinger proposed that interaction should be mediated by an intermediate vector boson [5], similar to the photon in QED.

$$\mathcal{L}_{\text{weak}} = \frac{G_F}{\sqrt{2}} \left(\bar{\psi}_p \gamma^\mu \psi_n\right) \left(\bar{\psi}_e \gamma^\mu \psi_\nu\right) \tag{1.1}$$

In 1958, the theoretical bases for the (V-A) structure of the weak interactions were formulated, this form represents a non-conservation of parity between the particles involved. In the same year, Bludman was the first to try to explain the weak interaction by assuming an invariance under a continuous group of transformations, using the $SU(2)$ symmetry [6]. His model contained interactions via charged-current, as well as neutral couplings, with the same strength and form that we see in current theories within a certain limit. However, the gauge theory of weak interactions alone is not renormalizable, requiring its unification with electromagnetic interactions into a single gauge theory.

With this in mind, in 1961 Glashow proposed a theory of unification of weak and electromagnetic interactions, combining them into a $SU(2)_L \otimes U(1)_Y$ symmetry group [7]. In this model there were two neutral mediators, the massless photon and the massive vector boson Z. However, the masses of mediating bosons and fermions have until now been placed ad hoc in the theories, without worrying about explaining where they come from. It was only in the late 60s, that Weinberg and Salam each independently proposed a mechanism for generating masses for the particles through a principle of gauge invariance and spontaneous symmetry breaking, known as the Higgs Mechanism [8, 9]. This mechanism predicts the existence of a scalar particle, the Higgs boson, and provides mass to the particles through the Higgs field.

In general, the main concepts that the SM is related to are group theory and Lie algebra, quantum field theory (QFT), as well as gauge invariance and spontaneous symmetry breaking. The idea of symmetry, or invariance of physical laws, is a fundamental concept not only for the SM but for theoretical physics in general. The importance of symmetries in QFT mainly stems from Noether's theorem, which succinctly states that: Every continuous symmetry of the action of a physical system with conservative forces has a corresponding conservation law [10]; a simple yet extremely powerful result. For example, if the system's Lagrangian is symmetric under continuous translations in space-time x^μ, this symmetry is related to the conservation of energy and linear momentum in the system, in the same way, in QED the conservation of eletric charge in a closed system is related to a unitary rotational symmetry of the field in the complex plane, also known as $U(1)_{EM}$ symmetry. The idea of symmetry is so fundamental in the SM that it is best known for its internal local symmetry group:

$$SU(3)_C \otimes SU(2)_L \otimes U(1)_Y \tag{1.2}$$

The symmetry group $SU(3)_C$ is related to the strong interaction, mediated by gluons, and C represents the conserved quantity in the symmetry, which is the **color charge**. This group has 8 generators, where each one corresponds to a gauge boson, in this case, the gluons of the model. On the other hand, $SU(2)_L \otimes U(1)_Y$ is the symmetry group related to the electroweak interactions, mediated by the photon, Z^0, and $W^\pm$ bosons, where each of these is a combination of the 4 generators of the groups, 3 from the SU(2) group and 1 from the U(1) group. The conserved quantity in the $SU(2)_L$ group is **weak isospin**, where L represents the left-handed

chirality of the interacting particles, while the conserved quantity in $U(1)_Y$ is **hypercharge**. In the SM only the symmetry of the electroweak group $SU(2)_L \otimes U(1)_Y$ is broken, hence its mediator bosons are combinations of the 4 generators of the group, something that does not happen with the $SU(3)_C$ group.

1.1 Elementary Particles

In the SM there are three types of elementary particles[1]: fermions, vector bosons, and a scalar boson. Fermions are semi-integer spin particles, which are also known as particles of matter, and are divided into two groups: Quarks and Leptons. Vector bosons are spin one gauge particles, and are known to be the mediators of the interactions between the particles of matter. Lastly, the Higgs boson, which is the only scalar boson in the SM, it has spin zero and is related to the Higgs field, which is responsible for giving mass to the particles.

The mathematical backgound used for the SM is QFT, and in QFT particles are described by fields $\phi(x)$, which in turn are functions of space-time coordinates $x \equiv x^\mu$ ($\mu = 0,1,2,3$), unlike wave functions in quantum mechanics (QM). Similar to classical field theory, the motion of particles as well as the interactions and potentials they undergo, are all described by a Lagrangian density[2] $\mathcal{L}(\phi(x), \partial_\mu \phi(x))$, where $\partial_\mu \phi(x)$ is the four-gradient of the field. The equations of motion for the system are obtained as solutions to the Euler-Lagrange equation for the Lagrangian density (1.4), such that this solution extremize the action S, as seen in Hamilton's principle.

$$S = \int_{t_1}^{t_2} dt L \equiv \int_{t_1}^{t_2} dt \int d^3x \mathcal{L}(\phi(x), \partial_\mu \phi(x)) \tag{1.3}$$

$$\frac{\partial \mathcal{L}}{\partial \phi(x)} - \partial_\mu \left(\frac{\partial \mathcal{L}}{\partial(\partial_\mu \phi(x))} \right) = 0 \tag{1.4}$$

1.1.1 Fermionic fields

As previously mentioned, fermions are particles with half-integer spin, which obey the Fermi-Dirac statistics, as well as Pauli's exclusion principle, meaning that only one fermion can occupy the same quantum state at a time. Free fermions are described by the free Dirac Lagrangian, that is, a Lagrangian without interaction terms, where ψ is the Dirac spinor representing the fermionic field and m is its respective mass:

$$\mathcal{L}_0 = \bar{\psi}(i\gamma^\mu \partial_\mu - m)\psi. \tag{1.5}$$

The symbol γ^μ represents the Dirac gamma matrices, whose properties are described in Appendix A.2, while the Dirac adjoint is defined as $\bar{\psi} = \gamma^0 \psi^\dagger$. In the Lagrangian, the term that involves

[1] Elementary particles are particles without internal structure.
[2] Lagrangian density will be abbreviated to Lagrangian in this work.

derivatives is called the kinetic term (Ex: $\bar{\psi} i\gamma^{\mu}\partial_{\mu}\psi$), while the term that involves only two fields is called mass term (Ex: $m\bar{\psi}\psi$).

Some of the characteristics of particles that are important for the following discussions have to do with their helicity and chirality. **Helicity** is the projection of spin in the direction of the particle's moment, if they are in the same direction the particle has right-handed helicity, and if they are in opposite directions the particle has left-handed helicity. **Chirality** is mathematical concept that is associated with Pauli matrices. These two concepts are different from each other, however, they are similar in relativistic regimes. For example, for a particle with mass the helicity is not well- defined, a boost on this particle can change the helicity from left to right, since the momentum depends on the coordinates, but the spin does not. However, for a massless particle, which is relativistic, if a particle has right-handed helicity in one frame of reference it will have it in all frames, that is, it will also be a chiral right-handed, and vice versa.

Regarding fermions in the SM, as discussed previously, they are divided into to two groups: quarks and leptons. The quarks are massive particles with a fractional electrical charge, and they are divided into three generations. In the first generation there is the up and down quarks, in the second one we have the charm and strange, and in the third one there is the top and bottom. Each generation of particles are arranged in left-handed doublets (L) and right-handed singlets (R):

$$\text{Quarks:} \quad \underbrace{\begin{pmatrix} u \\ d \end{pmatrix}_L, u_R, d_R,}_{1^{st}generation} \quad \underbrace{\begin{pmatrix} c \\ s \end{pmatrix}_L, c_R, s_R,}_{2^{nd}generation} \quad \underbrace{\begin{pmatrix} t \\ b \end{pmatrix}_L, t_R, b_R.}_{3^{rd}generation} \tag{1.6}$$

The left (L) and right (R) symbols refer to the chirality state of the fermion. We will address this aspect in more detail further below. In the same way as quarks, leptons are also divided into three generations, in the first we have the electron and the electron neutrino, in the second there is the muon and the muon neutrino, and in the third we have the tau and the tau neutrino. The electron, muon and tau are massive particles, and are known as charged leptons, as all three have an electrical charge $Q = 1$. Neutrinos are particles with zero electric charge and massless in the SM. Thus, there is no right-handed neutrino in the SM. Charged leptons coming in left-handed doublets and right-handed singlets:

$$\text{Léptons:} \quad \underbrace{\begin{pmatrix} \nu_e \\ e \end{pmatrix}_L, e_R,}_{1^{st}generation} \quad \underbrace{\begin{pmatrix} \nu_\mu \\ \mu \end{pmatrix}_L, \mu_R,}_{2^{nd}generation} \quad \underbrace{\begin{pmatrix} \nu_\tau \\ \tau \end{pmatrix}_L, \tau_R.}_{3^{rd}generation} \tag{1.7}$$

It is important to emphasize that each of these fermion particles has its respective anti-particle.

So far we have discussed the chirality of fermions, as well as showing that each of these particles can be divided into a right-handed and a left-handed part, now we will show how this is done mathematically and what physical implications this implies. If we define the chirality operators L and R and then we apply them to a fermion ψ we will obtain its left-handed and right-handed components respectively. We can decompose the field ψ as:

$$\psi = L\psi + R\psi = \psi_L + \psi_R, \tag{1.8}$$

where,

$$L \equiv \frac{1}{2}(1-\gamma^5) \quad ; \quad R \equiv \frac{1}{2}(1+\gamma^5). \tag{1.9}$$

The gamma matrix γ^5 is defined as $\gamma^5 = i\gamma^0\gamma^1\gamma^2\gamma^3$, with γ^i being the Dirac matrices (see Appendices A.2 and A.3. In terms of these chirality operators the fermion mass term is written as:

$$\begin{aligned} m\bar{\psi}\psi &= m(\bar{\psi}_L + \bar{\psi}_R)(\psi_L + \psi_R) \\ &= m(\bar{\psi}_L\psi_L + \bar{\psi}_L\psi_R + \bar{\psi}_R\psi_L + \bar{\psi}_R\psi_R) \\ &= m(\bar{\psi}\cancelto{0}{RL\psi} + \bar{\psi}RR\psi + \bar{\psi}LL\psi + \bar{\psi}\cancelto{0}{LR\psi}) \\ &= m(\bar{\psi}_L\psi_R + \bar{\psi}_R\psi_L). \end{aligned} \tag{1.10}$$

This means that for a fermion to have mass in the SM it must have the two chirality components ψ_L and ψ_R, which is why the neutrino has no mass in this model. This is an extremely important result because the fields ψ_L and ψ_R written above are considered as doublets. However only left-handed particles are arranged in doublets, meaning that mass terms of this type cannot arise in the SM. To solve this issue, a scalar field known as the Higgs doublet is introduced in these mass terms above, and it is this field that will be responsible for generating mass terms for the fermions.

Another important result occurs when we use these chirality properties in the fermionic weak charged-current, a current that represents interactions only between left-handed chirality fermions ψ_L, knowing the relation $\gamma^5\gamma^\mu = -\gamma^\mu\gamma^5$ we have that:

$$\begin{aligned} \bar{\psi}_L\gamma^\mu\psi_L &= \bar{\psi}R\gamma^\mu L\psi \\ &= \bar{\psi}\gamma^\mu L^2\psi \\ &= \frac{1}{2}\bar{\psi}\gamma^\mu(1-\gamma^5)\psi. \end{aligned} \tag{1.11}$$

the term $\gamma^\mu(1-\gamma^5)$ represents precisely the structure (V-A) of the charged-current, where V means the vector coupling (γ^μ) and A the axial coupling ($\gamma^\mu\gamma^5$). As previously stated, the beta decay which occurs via weak interaction, requires a structure of type (V-A) so that only neutrinos and left-handed electrons are generated in the decay.

Another important aspect is the fermion electric charges. As previously stated, the symmetry $SU(3)_C \otimes SU(2)_L \otimes U(1)_Y$ is associated with the conservation of color charge, Weak isospin[3] T^3, and Hypercharge Y, so that the last two are related to conservation of electric charge Q, from the Gell-Mann-Nishijima relationship:

$$Q = T^3 + \frac{Y}{2}. \tag{1.12}$$

These charges are directly related to the interactions between particles and their mediating bosons. Photons, for example, only mediate interactions between particles with an electrical charge, while $W^\pm$ bosons only interact with left-handed particles, that is, fermions with weak isospin. The charges of the respective fermions, as well as their general properties, are described in the following Table:

Particles	T^3	Y	Q
ν_e, ν_μ, ν_τ	+1/2	-1	0
e_L, μ_L, τ_L	-1/2	-1	-1
e_R, μ_R, τ_R	0	-2	-1
u_L, c_L, t_L	+1/2	+1/3	+2/3
d_L, s_L, b_L	-1/2	+1/3	-1/3
u_R, c_R, t_R	0	+4/3	+2/3
d_R, s_R, b_R	0	-2/3	-1/3

Table 1 – Properties of fermions in the SM.

One can show that the electric charge operator preserves the vacuum state and for this reason after spontaneous symmetry breaking, the electric charge is conserved generating the $U(1)$ electromagnetism group and consequently the Maxwell equations at low energies.

1.1.2 Bosonic fields

Vector Bosons are a class of particles that have spin one, in contrast to fermions, with half-integer spin. They follow Bose-Einstein statistics, which means that they are not subject to the Pauli exclusion principle and can occupy the same quantum state simultaneously, as in the Bose-Einstein condensate[4]. SM vector bosons are also gauge bosons, that is, they arise when we impose a local symmetry on the Lagrangian, so they are known to be the mediators of

[3] The Weak isospin T^3 is related to third Pauli matrix, with non-zero diagonal components, $T^3 = \tau_3/2$.

[4] The Bose-Einstein condensate represents the state of the system when the bosons are at extremely low temperatures, causing them to occupy the lowest energy state of the system at the same time.

interactions. The total number of mediating bosons is 12, where the electroweak interactions are mediated by a massless photon, two $W^{\pm}$, and one Z^0 both with mass; while the strong interactions are mediated by eight massless gluons.

As discussed previously, gauge bosons were first introduced in the context of the beta decay, as a way of trying to alleviate the problem of unitarity in the cross section in the Fermi effective theory. Furthermore, the need for bosons in the weak interaction to be massive comes from the fact that the distance of the interaction is inversely proportional to the mass of the particles that mediate it. For example, in the case of electromagnetic interactions the photon has no mass, and therefore the interaction occurs at infinite distances, while the massive bosons $W^{\pm}$ and Z^0 of the weak interaction interact at a short distance. The case of gluons is special, despite having no mass, the quarks that interact strongly are not found free in nature, always forming baryons and mesons. In other words, quarks are confined in hadrons. Confinement is essential to explain why nuclear forces have very short range while massless gluon exchange would be long range. Nucleons are color singlets and consequently, they cannot exchange gluons but only colorless states. The lightest color singlet hadronic particles are pions. So the range of nuclear forces is fixed by the pion mass, $r \sim m_{\pi}^{-1} \sim 10^{-13} cm$, which is short range. A table with the properties and interactions of each gauge boson in the standard model can be seen below:

Boson	Interaction	Mass	Q
Photon	Eletromagnetic	0	0
Z	Weak	91.1876±0.0021 GeV	0
W	Weak	80.377±0.012 GeV	±1
Gluon	Strong	0	0

Table 2 – Properties of bósons in the SM.

These spin one vector bosons, also known as gauge fields, have their dynamics described by the Proca Lagrangian. Considering a local gauge theory $U(1)$, for a single massless gauge field A_μ with field-strength tensor $F^{\mu\nu}$, we have that this Lagrangian is:

$$\mathcal{L} = -\frac{1}{4} F_{\mu\nu} F^{\mu\nu}, \tag{1.13}$$

where

$$F_{\mu\nu} = \partial_\nu A_\mu - \partial_\mu A_\nu. \tag{1.14}$$

The only term in the lagrangian is called the kinetic term, as it describes the dynamics of the vector field A_μ, while a mass term of the type $m^2 A_\mu A^\mu$ was not included because it is incompatible with local gauge symmetry. For QED, which is a $U(1)$ theory with the massless photon as a mediating boson, this is not a problem; but if we wish to explain short-range

interactions like the weak interaction, which involves massive bosons, then a local gauge theory creates a problem, which is solved by Higgs mechanism.

1.1.3 Scalar fields

The only particle in the standard model described by a scalar field ϕ is the Higgs boson ($\phi = h$), it has zero electric charge, a mass of 125.11±0.11 GeV, and because it is a scalar boson it has zero spin and obeys the Bose-Einsten statistics. Unlike other SM particles, the Higgs boson interacts with particles based on a coupling that is proportional to the mass of the particle itself, so that the interaction is stronger for particles with more mass and is zero for massless particles, like the photon. Scalar bosons have their dynamics described by the Klein-Gordon Lagrangian, considering real scalar fields such as the Higgs boson h, the Lagrangian is given by:

$$\mathcal{L} = \frac{1}{2}\left[(\partial_\mu \phi)(\partial^\mu \phi) - m^2\phi^2\right]. \tag{1.15}$$

Where as usual the first term is the kinetic term and the second is the mass term. If we consider a complex field (1.17), which has two components, a real ϕ_1 and an imaginary ϕ_2, the Klein-Gordon Lagrangina is given by:

$$\mathcal{L} = (\partial_\mu \phi)^*(\partial^\mu \phi) - m^2\phi^*\phi, \tag{1.16}$$

where

$$\phi = \frac{\phi_1 + i\phi_2}{\sqrt{2}}. \tag{1.17}$$

Another important aspect, especially for SM, is the construction of the potential term $V(\phi)$ for a complex scalar field, so that:

$$\mathcal{L} = (\partial_\mu \phi)^*(\partial^\mu \phi) - V(\phi^*\phi). \tag{1.18}$$

Where this potential term is used in the context of the Higgs mechanism to spontaneously break the $SU(2) \times U(1)$ symmetry and generate mass for the particles. This potential term is given by:

$$V(\phi^*\phi) = \mu^2\phi^*\phi + \lambda(\phi^*\phi)^2, \tag{1.19}$$

so that μ^2 and λ at first glance are constants, and μ has an energy dimension. It will be seen later that this μ^2 actually varies, and it is this variation that generates the spontaneous breaking of the symmetry.

1.2 Gauge invariance

We have addressed gauge symmetries and their role in explaining the fundamental interactions of nature, but we haven't yet described how this happens. Consider an object possessing some form of symmetry that remains unchanged under a specific transformation, for example, when we rotate a symmetric sphere its shape remains constant. This principle extends to physical systems, where certain symmetries in the system allows for transformations that leave its equations of motion unaltered. The idea of keeping the laws of physics invariant under transformations has been around for some time, but it gained significant attention with Maxwell's electrodynamics. In 1864, Maxwell successfully unified electrical and magnetic interactions within a single framework. Utilizing these equations, its possible to define electric and magnetic fields using potentials that do not have unique definitions. In other words, numerous potentials can describe the same physical fields, and this flexibility (invariance) in selecting potentials has become known as gauge invariance.

Currently, the concept of gauge invariance is more generic, and it is related to continuous symmetries of the Lagrangian. This invariance is associated with two types of gauge transformations: global and local. **Global transformations** are applied uniformly to all points of the system with the same intensity. If the system's Lagrangian is invariant under this type of transformation, it is possible to find its corresponding conserved current through Noether's theorem. On the other hand, **local transformations** are functions of the system's physical coordinates x^{μ}, making their application nontrivial. If we impose that the Lagrangian is invariant under this type of transformation, some important results can arise, such as interaction terms between gauge bosons and matter.

As we are interested in transformations and symmetries related to subatomic particles, we must study them taking into account the properties of quantum mechanics (QM). Wigner's theorem says that in Hilbert space, physical symmetries can be represented mathematically by unitary operators [11], which means that given a continuous local transformation U(x), it must obey the following relationship:

$$U^{\dagger}U = UU^{\dagger} = 1. \tag{1.20}$$

This type of property is important as it preserves **unitarity**, ensuring that probability is conserved. Another important property of the transformation is that it must be a **proper transformation**, meaning $det(U) = 1$. This is done so that when U is applied, it does not alter the physical dimensions or scale of the system. In group theory, a group in which the elements have these characteristics is called a special unitary group[5] $SU(n)$, a group composed of $n \times n$ matrices,

[5] The special unitary group is a type of Lie group, which is a group with continuous and differentiable elements, therefore being perfect for describing continuous symmetries.

and with dimension $n^2 - 1$ which is also to the number of generators of the group. An example of an element from this group expanded in a Taylor series is:

$$U(x) = exp\,(ig\alpha^a(x)T^a) \approx 1 + ig\alpha^a(x)T^a + ... \tag{1.21}$$

Where T^a represents the group's generators, $\alpha^a(x)$ are infinitesimal functions of the physical coordinates x^μ, and g is the coupling constant. The set of generators forms a vector space, and the elements of this space can be related to each other through an algebra, if this algebra is a commutator it is known as a Lie algebra, and is given by:

$$[T^a, T^b] = i\varepsilon^{abc}T^c, \tag{1.22}$$

where ε^{abc} is the structure constant of the group, and its elements are antisymmetric. If the commutator of the group's generators is zero ($\varepsilon^{abc} = 0$) the algebra is said **abelian**, if they do not comult ($\varepsilon^{abc} \neq 0$) the algebra is **non-abelian**. This characteristic of the generators has a very important physical consequence, which is the self-interaction between the gauge bosons in a process. If the bosons are generated by an abelian group they do not interact with each other (like photons), and if they are related to a non-abelian group they interact (like gluons). The exact way how this happens will be seen below.

1.2.1 Yang–Mills theories

Historically, the Yang-Mills theory was a theory developed by C. Yang and R. Mills in 1954 to explain strong interactions in the atomic nucleus [12], with the isospin as the conserved quantity[6]; this theory was mainly inspired by the famous QED, where the conserved quantity is the electrical charge. However, unlike QED which is an abelian $U(1)_{EM}$ theory, the Yang-Mills theory sought to explain nuclear phenomena from a non-abelian $SU(2)$ local gauge theory. This theory proved so important that it was later used as a basis for describing theories such as the unification of the electroweak interactions $SU(2) \times U(1)$, and the strong interaction it self $SU(3)$, also known as quantum chromodynamics (QCD). Because it is such a relevant type of theory for the description of fundamental interactions, the term Yang-Mills theories currently refers to any class of gauge theory which is local and non-abelian.

With this in mind, to better understand how this type of theory works we consider as an example the free Dirac lagrangian for fermions (1.5):

$$\mathcal{L}_0 = \bar{\psi}(i\gamma^\mu\partial_\mu - m)\psi. \tag{1.23}$$

[6] Historically the isospin is a quantum number used to differentiate the proton from the neutron (if you ignore their electrical charges and small diference in mass), but today we consider the fractional isospin at the level of quarks and leptons.

If we apply a global transformation $\boldsymbol{\alpha} \neq \boldsymbol{\alpha}(x)$ to the ψ field, or rotation in the isospin space (1.24), we can see that the Lagrangian does not vary $\delta\mathcal{L} = 0$, therefore, according to Noether's theorem we can find a conserved isospin current density $\partial_\mu \mathbf{J}^\mu = 0$, so that:

$$\psi \rightarrow \psi' = exp\left(\frac{i\boldsymbol{\alpha}\cdot\boldsymbol{\tau}}{2}\right)\psi, \tag{1.24}$$

$$\mathbf{J}^\mu = \bar{\psi}\gamma^\mu\frac{\boldsymbol{\tau}}{2}\psi. \tag{1.25}$$

Where the object $\boldsymbol{\tau} = (\tau_1, \tau_2, \tau_3)$ has as components the 2×2 Pauli isospin matrices[7]. However, if we consider a local transformation $\boldsymbol{\alpha} = \boldsymbol{\alpha}(x)$ in the field ψ, the lagrangian will no longer be invariant $\delta\mathcal{L} \neq 0$, since $\partial_\mu\psi'$ will present extra terms due to the dependence on the physical coordinates of the partameter $\boldsymbol{\alpha}(x)$. Therefore, if we want to force the lagranginan to also be invariant under local transformations, we must modify the covariant derivative to a gauge-covariant one [13]:

$$\partial_\mu \rightarrow \mathcal{D}_\mu = I\partial_\mu + igB_\mu, \tag{1.26}$$

so that $B_\mu = \frac{1}{2}\boldsymbol{\tau}\cdot\mathbf{b}_\mu = \frac{1}{2}\tau_a b^a_\mu$, where $\mathbf{b}_\mu$ is the isovector whose components are the three gauge bosons of the theory $\mathbf{b}_\mu = (b^1_\mu, b^2_\mu, b^3_\mu)$. Knowing this, we have that:

$$B_\mu = \begin{pmatrix} b^3_\mu & b^1_\mu - ib^2_\mu \\ b^1_\mu + ib^2_\mu & -b^3_\mu \end{pmatrix}. \tag{1.27}$$

It is also important to note that for each gauge boson b^a_μ there is an associated generator τ^a, so if we are working with the $SU(2)$ group, where $n = 2$, the number of gauge bosons in the theory is equal to the dimension of the group: $n^2 - 1 = 3$. In addition to the modification in the covariant derivative, to guarantee local invariance it is also necessary that the gauge bosons are modified, so that they transform as:

$$b'^a_\mu = b^a_\mu - \frac{1}{g}\partial_\mu\alpha^a - \varepsilon_{abc}\alpha^b b^c_\mu. \tag{1.28}$$

As seen previously, the term ε_{abc} is the group structure constant. If the gauge field b^a_μ transforms so that $\varepsilon_{abc} \neq 0$, then the nature of the isospin rotation is that of a non-Abelian symmetry group, as expected. If we apply the gauge-covariant derivative (1.26) to the Dirac Lagrangian (1.23):

[7] The generators of the $SU(2)$ group are functions of the Pauli isospin matrices, so that these generators are given by $T^a = \tau_a/2$.

$$\begin{aligned}\bar{\psi}(i\gamma^\mu \mathcal{D}_\mu - m)\psi &= \bar{\psi}(i\gamma^\mu[\partial_\mu + igB_\mu] - m)\psi \\ &= \mathcal{L}_0 - g\underbrace{\left(\bar{\psi}\gamma^\mu \frac{\boldsymbol{\tau}}{2}\psi\right)}_{\mathbf{J}^\mu} \cdot \mathbf{b}_\mu = \mathcal{L}_0 - \frac{g}{2}\bar{\psi}\gamma^\mu \tau^a \psi b^a_\mu,\end{aligned} \tag{1.29}$$

we will obtain the free Dirac lagrangian itself $\mathcal{L}_0$, and interaction terms between the fermions ψ and each of the three gauge bosons b^a_μ, so that the nature of this interaction term is the same conserved isospin current seen in (1.25). It's worth emphasizing that these interaction terms arise due to the locality of the gauge transformation.

With this we can describe well how the field ψ behaves, as well as its interaction with the gauge bosons b^a_μ, however we still do not know how the bosonic fields themselves $b^a{}_{mu}$ behave. To describe this we use the proca Lagrangian (1.13), which is equivalent to a free bosonic field. Just as the object B_μ is decomposed into components when we work with a $SU(2)$ symmetry, so is the field-strength tensor $F_{\mu\nu}$, in a way that $F_{\mu\nu} = \frac{1}{2}\boldsymbol{\tau} \cdot \mathbf{F}_{\mu\nu} = \frac{1}{2}\tau_a F^a_{\mu\nu}$. In this way, the invariant kinetic term of the Proca Lagrangian becomes[8]:

$$\mathcal{L} = -\frac{1}{4}\mathbf{F}_{\mu\nu} \cdot \mathbf{F}^{\mu\nu} = -\frac{1}{4}F^a_{\mu\nu}F^{\mu\nu}_a = -\frac{1}{2}\mathrm{tr}(F_{\mu\nu}F^{\mu\nu}). \tag{1.30}$$

where

$$F_{\mu\nu} = -\frac{i}{g}[\mathcal{D}_\nu, \mathcal{D}_\mu] = \partial_\nu B_\mu - \partial_\mu B_\nu + ig[B_\nu, B_\mu], \tag{1.31}$$

the last term arises so that $F_{\mu\nu}$ is invariant under the imposed local gauge transformation; in addition, this term is responsible for the self-interaction between the gauge bosons in the theory. To understand how this happens, we write the components of the field-strength tensor $F^a_{\mu\nu}$, so that the fields b^a_μ are made explicit, so that:

$$F^a_{\mu\nu} = \partial_\nu b^a_\mu - \partial_\mu b^a_\nu + g\epsilon_{abc}b^b_\mu b^c_\nu. \tag{1.32}$$

If we open the kinetic term (1.30) by expanding the field-strength components (1.32) we will have [14]:

$$\begin{aligned}\mathcal{L} = -\frac{1}{4}F^a_{\mu\nu}F^{\mu\nu}_a &\propto (\partial_\nu b_\mu - \partial_\mu b_\nu + g b_\mu b_\nu)(\partial^\nu b^\mu - \partial^\mu b^\nu + g b^\mu b^\nu) \\ &= \underbrace{(\partial_\nu b_\mu - \partial_\mu b_\nu)^2}_{\text{Kinetic}} - \underbrace{g(\partial_\nu b_\mu - \partial_\mu b_\nu)b^\mu b^\nu + ...}_{\text{Triple}} + \underbrace{g^2 b_\mu b_\nu b^\mu b^\nu}_{\text{Quartic}}.\end{aligned} \tag{1.33}$$

[8] In this step the Pauli-matrix identity was used: $\mathrm{tr}(\tau^a\tau^b) = 2\delta^{ab}$.

Where the kinetic (or propagator) term appear, as well as terms of triple and quartic interactions between the gauge bosons of the theory. These interactions only arise because the symmetry group used is non-abelian, so that if the group structure constant were to be zero these interactions would never appear.

Another important characteristic to be studied about these Yang-Mills's bosons is their mass term. Considering the term $m^2 b^a_\mu b^{a\mu}$, if we want to know if it is invariant under rotations in the isospin space we must apply the gauge transformation (1.28) to it, so that:

$$\begin{aligned} b'^{a}_{\ \mu} b'^{\mu}_{\ a} &= \left(b^a_\mu - \frac{1}{g}\partial_\mu \alpha^a - \varepsilon_{abc}\alpha^b b^c_\mu \right) \left(b^{a\mu} - \frac{1}{g}\partial^\mu \alpha^a - \varepsilon_{apq}\alpha^p b^{q\mu}. \right) \\ &\neq b^a_\mu b^\mu_a. \end{aligned} \tag{1.34}$$

Therefore, we can clearly see that a mass term for this type of boson is not invariant under the gauge transformation, meaning that these bosons cannot have mass. This was a big problem for the original Yang-Mills theory, because as previously stated it was a theory created to describe strong interactions in the atomic nucleus, and as these interactions occur at short distances, it was imagined at the time that whatever this interaction mediators is they should be massive [15]. Therefore, if we wish to use a Yang-Mills theory to explain interactions mediated by massive bosons, then we must turn our attention to the famous Higgs mechanism.

1.3 Higgs Mechanism

The Higgs mechanism is based on the concept of spontaneous symmetry breaking (SSB), which occurs when the system's Lagrangian is symmetric under a certain transformation, but its vacuum state is not. A classic example of this phenomenon is the magnetization of an infinite ferromagnetic material: at a high enough temperature, the magnetic dipoles of this material will be misaligned, making the system symmetric under three-dimensional rotations $SO(3)$; but as the temperature decreases below the Curie temperature T_c, the dipoles will align in a random direction, breaking the $SO(3)$ symmetry and transforming it into a two-dimensional rotational symmetry $SO(2)$ around the total magnetization direction of the system. The randomness in the direction of the total magnetization represents a degenerate minimum energy state (vacuum state), and the choice of a direction represents the breaking of the previous symmetry and the emergence of a new one. A similar process occurs with the gauge symmetries in our universe.

An important consequence of a SSB arises from the Goldstone's theorem [16], which states that one massless spin-zero particle called a Goldstone will occur for each broken generator of the original symmetry group, where each of these Goldstones represents a degree of freedom in the system. If the broken symmetry is a local gauge symmetry, the degrees of freedom of the Goldstones are "eaten"by the massless gauge bosons, so that these bosons gain an extra

degree of freedom in the form of a longitudinal polarization component, representing a mass for these gauge bosons. This process of generating mass for the gauge bosons is called the Higgs mechanism.

To understand how this mechanism works, we first see how goldstones are generated in a SSB. Consider a complex scalar field $\phi = \frac{\phi_1 + i\phi_2}{\sqrt{2}}$ which is described by the Lagrangian:

$$\mathcal{L} = (\partial_\mu \phi)^* (\partial^\mu \phi) - V(\phi^* \phi). \tag{1.35}$$

Firstly, we make this Lagrangian invariant under the global transformations (1.36), in this case the potential can only have even terms; furthermore, we will only consider terms up to the fourth order, so that the theory is renormalizable, this gives us:

$$\phi \to \phi' = e^{i\theta}\phi, \tag{1.36}$$

$$V(\phi^* \phi) = \mu^2 \phi^* \phi + \lambda(\phi^* \phi)^2. \tag{1.37}$$

The quartic term of the potential has $\lambda > 0$ to ensure stability against unbounded oscillations, however the quadratic term can have in principle μ^2 with either positive or negative values. If $\mu^2 > 0$, the expected value of the theory's vacuum will be $\langle \phi \rangle_0 = 0$, which is a well-defined and symmetric minimum. Furthermore, in this situation both ϕ_1 and ϕ_2 fields will have mass terms, as can be seen by expanding the potential (1.37) in (1.35) with respect to these fields:

$$\mathcal{L} = \frac{1}{2}(\partial_\mu \phi_1)(\partial^\mu \phi_1) + \frac{1}{2}(\partial_\mu \phi_2)(\partial^\mu \phi_2) - \frac{\mu^2}{2}\phi_1^2 - \frac{\mu^2}{2}\phi_2^2 + ... \tag{1.38}$$

On the other hand, if $\mu^2 < 0$ the system will present infinitely many possible values for the minimum (1.39), so that all vacuum states in the theory have the same degenerate energy, as shown in Figure 1.

$$\langle \phi^2 \rangle_0 = \frac{1}{2}\left[\langle \phi_1^2 \rangle_0 + \langle \phi_2^2 \rangle_0\right] = -\frac{\mu^2}{2\lambda} \equiv \frac{v^2}{2}, \tag{1.39}$$

the constant v can be understood as the energy of the vacuum, which defines the location of the degenerate vacuum from a combination of the fields ϕ_1 and ϕ_2, thus forming a ring with the possible minimums of the potential. This degenerate configuration arises due to the rotational symmetry $SO(2)$ of the potential. We can choose any point on the ring to be the physical vacuum of the theory, as long as the fields ϕ_1 and ϕ_2 satisfy the relation (1.39). When this choice is made, the potential will no longer be symmetric with respect to the theory's minimum, thus representing a spontaneous breaking of the $SO(2)$ symmetry. Our choice of the minimum will be made such that one of the fields develops a vacuum expectation value (VEV) while the other

does not, so that we will have $\langle\phi_1\rangle_0 = v$ and $\langle\phi_2\rangle_0 = 0$. In this new minimum, the VEV of the complex field is not zero but rather $\langle\phi\rangle_0 = v/\sqrt{2}$. To maintain this value as zero, we will choose a new parameterization of the fields, such that:

$$\phi' = \phi - \frac{v}{\sqrt{2}} \qquad \Longrightarrow \qquad \begin{cases} \eta = \phi_1 - v \\ \zeta = \phi_2 \end{cases} \tag{1.40}$$

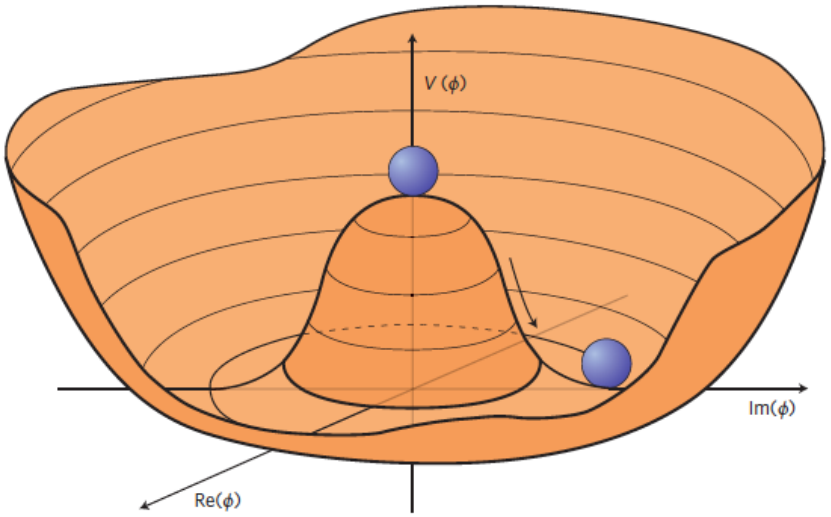

Figure 1 – Representation of the complex scalar potential for the case where $\mu^2 < 0$. In this situation the vacuum state is described by a randomlychosen point around the valley of the potential [17].

Applying this transformation in to the Lagrangian (1.35) and considering that $v^2 = -\frac{\mu^2}{\lambda}$, we find that:

$$\mathcal{L} = \frac{1}{2}(\partial_\mu\eta)(\partial^\mu\eta) + \frac{1}{2}(\partial_\mu\zeta)(\partial^\mu\zeta) - \frac{1}{2}(-2\mu^2)\eta_1^2 + ... \tag{1.41}$$

Note that both fields had mass terms before (1.38), but now only the field η that developed a VEV has mass, with $m^2 = -2\mu^2 > 0$, while the second field ζ that did not develop a VEV became a goldstone. The mass of the η field can be understood as a consequence of the potential's restoring force, as it oscillates radially. However, the ζ field lacks mass because it oscillates angularly in a direction where the potential remains invariant.

So far we have only made mathematical comments regarding the sign of the parameter μ^2, however this change in sign has a profound physical meaning. This parameter is actually a function of the temperature of the universe T, such that for very high temperatures at the beginning of the universe $\mu^2(T) > 0$, and as the universe expanded and its temperature decreased the parameter became $\mu^2(T) < 0$, thus triggering a SSB in the universe.

Now that we have shown how an SSB can generate goldstones that turn into degrees of freedom in the lagrangian, we explain how those degrees of freedom make gauge bosons massive

fields. Consider a local and Abelian gauge theory, in this theory the lagrangian (1.35) must be invariant under a local transformation in the form:

$$\phi' = e^{iq\alpha(x)}\phi. \tag{1.42}$$

As seen previously, to guarantee this invariance the derivative must be transformed into a gauge-covariant derivative, in addition the gauge field must also change, so that:

$$D_\mu = \partial + iqA_\mu \tag{1.43}$$

$$A'_\mu = A_\mu - \partial_\mu \alpha(x) \tag{1.44}$$

Therefore, the lagrangian that describes the scalar field ϕ, the gauge field A_μ, and the interactions between them is given by:

$$\mathcal{L} = (D_\mu\phi)^*(D^\mu\phi) - V(\phi^*\phi) - \frac{1}{4}F_{\mu\nu}F^{\mu\nu}. \tag{1.45}$$

As done before, we will consider a SSB such that $\mu^2 < 0$. In this situation the VEV of the fields will be $\langle\phi\rangle_0 = v/\sqrt{2}$, again we will choose $\langle\phi_1\rangle_0 = v$ and $\langle\phi_2\rangle_0 = 0$. For the VEV of the complex field to remain zero, we consider a convenient parameterization which is given by:

$$\phi = \frac{e^{i\zeta/v}(\eta + v)}{\sqrt{2}} \approx \frac{1}{\sqrt{2}}(\eta + v + i\zeta). \tag{1.46}$$

This parameterization is equivalent to the previous one (1.40), and represents small oscillations of the η and ζ fields around the vacuum. Applying the parameterization (1.46) to the lagrangian (1.45), we find:

$$\begin{aligned}\mathcal{L} =& \frac{1}{2}[(\partial_\mu\eta)(\partial^\mu\eta) - (-2\mu^2)\eta^2] + \frac{1}{2}[(\partial_\mu\zeta)(\partial^\mu\zeta)] \\ &- \frac{1}{4}F_{\mu\nu}F^{\mu\nu} + qvA_\mu(\partial^\mu\zeta) + \frac{q^2v^2}{2}A_\mu A^\mu + ...\end{aligned} \tag{1.47}$$

The field A_μ is not yet a physical field, as it has the mass term mixed with the field ζ[9]. To solve this we can rewrite the last two terms in combination with the kinetic term of ζ and find the relationship:

$$\frac{q^2v^2}{2}\left(A_\mu + \frac{1}{qv}\partial_\mu\zeta\right)\left(A^\mu + \frac{1}{qv}\partial^\mu\zeta\right). \tag{1.48}$$

[9] The states of interaction of the fields A_μ and ζ are not their mass states.

This is equivalent to making a new transformation in the field A_μ, in order to create a mass term for it. This transformation can be done using the degree of freedom in the parameter α of the gauge transformation (1.44), so that $\alpha = -\zeta/qv$, thus the transformation of A_μ is in the form:

$$A'_\mu = A_\mu + \frac{1}{qv}\partial_\mu \zeta. \tag{1.49}$$

Therefore, the local transformation of the field that we had previously (1.42) now, after a SSB, takes the form:

$$\phi' = e^{iq\alpha(x)} e^{i\zeta/v} \frac{(\eta + v)}{\sqrt{2}} = \frac{(\eta + v)}{\sqrt{2}}. \tag{1.50}$$

This choice for the value of the α parameter is called a unitary gauge, which is the gauge where the goldstones disappear after a SSB. Substituting the relations (1.50) and (1.49) into the lagrangian (1.47) we find:

$$\mathcal{L} = \frac{1}{2}[(\partial_\mu \eta)(\partial^\mu \eta) - (-2\mu^2)\eta^2] - \frac{1}{4}F_{\mu\nu}F^{\mu\nu} + \frac{q^2 v^2}{2}A'_\mu A'^\mu + ... \tag{1.51}$$

Therefore, we can see that after a SSB, the degree of freedom of the Goldstone can be absorbed by the gauge boson, giving rise to a longitudinal polarization component, which is equivalent to giving mass to the boson, thus characterizing the Higgs mechanism. This implies that if we want to generate mass for the gauge bosons of the Standard Model, we must include scalar fields in this model.

1.4 Electroweak Theory

So far, we have described the particle content of the SM in addition to its main characteristics, demonstrated how to use the principle of gauge invariance to describe interactions between matter and the mediating bosons, and finally shown the necessity of the existence of a scalar field in the model to give mass to both the gauge bosons and the massive fermions in nature.

From now on, we will focus our discussions on the Lagrangian that describes the electroweak interaction in the SM. This Lagrangian is usually divided into sectors, where each sector is responsible for a function in the model, such as describing propagation, interactions, and generating mass for the particles. This sector-divided Lagrangian is given by:

$$\mathcal{L}_{Weak} = \mathcal{L}_{Scalar} + \mathcal{L}_{Gauge} + \mathcal{L}_{Fermions} + \mathcal{L}_{Yukawa}. \tag{1.52}$$

This theory obeys the symmetry $SU(2)_L \times U(1)_Y$, where the generators of the $SU(2)_L$ group are given by $\tau^a/2$, and each of them is associated with its respective gauge boson (1.53).

The generator of the $U(1)_Y$ group on the other hand is the hypercharge $Y/2$, which is associated with the gauge boson (1.54). It is worth noting that these gauge bosons are not physical, later it will be shown that the physical bosons are, in fact, written as combinations of these.

$$SU(2)_L: \quad W_\mu^1,\ W_\mu^2,\ W_\mu^3, \tag{1.53}$$

$$U(1)_Y: \quad B_\mu. \tag{1.54}$$

Furthermore, each gauge boson is associated with a component of its respective strength tensor, which in this case are given by:

$$\begin{aligned} W_{\mu\nu}^a &= \partial_\nu W_\mu^a - \partial_\mu W_\nu^a + g\epsilon_{abc} W_\mu^b W_\nu^c, \\ B_{\mu\nu} &= \partial_\nu B_\mu - \partial_\mu B_\nu. \end{aligned} \tag{1.55}$$

As can be seen in Table 1, right-handed fermions do not possess weak isospin like the left-handed ones, which means that they do not interact with the gauge bosons associated with the $SU(2)_L$ symmetry. However, fermions of both chiralities have hypercharge, interacting with the gauge boson associated with the $U(1)_Y$ symmetry. Thus, if we want the Lagrangian (1.52) to be locally invariant, we must adopt a gauge covariant derivative that acts differently for left-handed and right-handed fermions, such that:

$$\begin{aligned} \text{Left-hand:} \quad & D_\mu = \partial_\mu + i\frac{g'}{2} Y B_\mu + i\frac{g}{2}\tau_a W_\mu^a; \\ \text{Right-hand:} \quad & D_\mu = \partial_\mu + i\frac{g'}{2} Y B_\mu. \end{aligned} \tag{1.56}$$

Where g' and g are the coupling constants associated with the $U(1)_Y$ and $SU(2)_L$ symmetries, respectively. Furthermore, as discussed earlier, the fermions of the SM can be separated into left-handed (L) and right-handed (R) components. In the case of leptons, the notation used to describe their chiralities will be:

$$L_l \equiv \begin{pmatrix} \nu_l \\ l \end{pmatrix}_L = \begin{pmatrix} L\nu_l \\ Ll \end{pmatrix} = \begin{pmatrix} \nu_{lL} \\ l_L \end{pmatrix} \quad ; \quad R_l \equiv l_R \tag{1.57}$$

.

The label l represents the lepton generation, so that $l = e, \mu, \tau$. For quarks, we will consider the notation $U_i = u, c, t$ for the up-like quarks, and $D_i = d, s, b$ for the down-like quarks. Their chirality components are described as:

$$L_i \equiv \begin{pmatrix} U_i \\ D_i \end{pmatrix}_L = \begin{pmatrix} U_{iL} \\ D_{iL} \end{pmatrix} \quad ; \quad R_{U_i} \equiv U_{iR} \quad ; \quad R_{D_i} \equiv D_{iR}. \tag{1.58}$$

.

With these general considerations about the electroweak model in mind, we will now describe each of the sectors of its Lagrangian (1.52), starting with the scalar sector.

1.5 Scalar sector

The Lagrangian of the scalar sector is responsible for giving mass to the gauge bosons and the Higgs boson, as well as generating the interaction terms between them. It was shown in the Higgs mechanism that the Goldstones generated in spontaneous symmetry breaking (SSB) represent degrees of freedom that can be absorbed by the gauge bosons to give them mass. In the case of electroweak interaction, it is mediated by three massive bosons and one massless boson, so the SSB must generate three Goldstones. To achieve this, the formalism of the Higgs doublet (1.59) is used, which is an object formed by two complex scalar fields, each with two components (one real and one imaginary), totaling four real scalar fields. Three of these fields will be the Goldstones of the theory, while the last will become the Higgs boson.

$$\phi = \begin{pmatrix} \phi^+ \\ \phi^0 \end{pmatrix} \qquad \Longrightarrow \qquad \phi = \frac{1}{\sqrt{2}} \begin{pmatrix} \phi_1 + i\phi_2 \\ \phi_3 + i\phi_4 \end{pmatrix}. \tag{1.59}$$

This form of the Higgs doublet, with a charged field ϕ^+ and a neutral field ϕ^0, is necessary for the terms in the Yukawa Lagrangian to have a total electric charge equal to zero. Furthermore, if we want to satisfy the electric charge operator (1.12), we must set the hypercharge of the Higgs doublet to be $Y_\phi = +1$. With this in mind, the form of the scalar sector Lagrangian is given by:

$$\mathcal{L}_{Scalar} = (D_\mu \phi)^\dagger (D^\mu \phi) - V(\phi^\dagger \phi), \tag{1.60}$$

where

$$V(\phi^\dagger \phi) = \mu^2 \phi^\dagger \phi + \lambda (\phi^\dagger \phi)^2. \tag{1.61}$$

At this point we have already considered that the Lagrangian is invariant under $SU(2)_L \times U(1)_Y$, so that the gauge covariant derivative is given by (1.56). For $\mu^2 < 0$, we can choose the VEV of the Higgs field to be:

$$\langle \phi \rangle_0 = \frac{1}{\sqrt{2}} \begin{pmatrix} 0 \\ v \end{pmatrix}. \tag{1.62}$$

This choice must be made in such a way that the charged field does not generate a VEV, as this would violate the conservation of electric charge. Up to this point, we have been very careful to ensure that electric charge is conserved, because this conservation is a consequence of the

electromagnetic symmetry we currently observe in nature, so this is a symmetry that must emerge after the SSB. This is equivalent to saying that after the breaking of the old symmetry, the new vacuum of the theory must be invariant under $U(1)_{EM}$, which conserves electric charge:

$$SU(2)_L \times U(1)_Y \quad \longrightarrow \quad U(1)_{EM}.$$

After choosing the VEV of the Higgs field, we select a new parameterization so that the new field is equivalent to small perturbations around the vacuum, and in order for the Goldstones to disappear, we can use the unitary gauge, giving us:

$$\phi = \frac{(v+h)}{\sqrt{2}} \begin{pmatrix} 0 \\ 1 \end{pmatrix}, \tag{1.63}$$

where h represents the Higgs boson. Applying the new field (1.63) and the invariant covariant derivative (1.56) to the scalar sector Lagrangian (1.60), we find that:

$$\begin{aligned} \mathcal{L}_{Scalar} = & \left| \left(\partial_\mu + i\frac{g'}{2} Y B_\mu + i\frac{g}{2}\tau_a W_\mu^a \right) \frac{(v+h)}{\sqrt{2}} \begin{pmatrix} 0 \\ 1 \end{pmatrix} \right|^2 \\ & - \mu^2 \frac{(v+h)^2}{2} - \lambda \frac{(v+h)^4}{4}. \end{aligned} \tag{1.64}$$

1.5.1 Masses of the electroweak gauge bosons

Looking only at the kinetic term in (1.64), if we expand it considering the definition of the Pauli matrices described in Appendix A.1, and that $Y_\phi = +1$, we will have:

$$\mathcal{L}_{Scalar} \supset \left| \begin{pmatrix} 0 \\ \partial_\mu h/\sqrt{2} \end{pmatrix} + \frac{i}{2}(v+h) \begin{pmatrix} \frac{g(W_\mu^1 - iW_\mu^2)}{\sqrt{2}} \\ \frac{(g'B_\mu - gW_\mu^3)}{\sqrt{2}} \end{pmatrix} \right|^2, \tag{1.65}$$

so that

$$\mathcal{L}_{Scalar} \supset \frac{1}{2}\partial_\mu h \partial^\mu h + \frac{(v+h)^2}{8} \left[g^2 |W_\mu^1 - iW_\mu^2|^2 + |g'B_\mu - gW_\mu^3|^2 \right]. \tag{1.66}$$

In this situation, to generate bosons with well-defined mass terms, that is, physical bosons, we can consider the redefinition:

$$W_\mu^\pm = \frac{W_\mu^1 \mp iW_\mu^2}{\sqrt{2}}, \tag{1.67}$$

This results in mass terms for the charged bosons $W^{\pm}$ in Equation (1.66). However, for the last term, the situation is different, as it is a mixing term with different couplings g and g', so other methods are needed to make the physical bosons explicit. First, we can rewrite the term as the result of a matrix product [18]:

$$\begin{pmatrix} B^{\mu} & W^{3\mu} \end{pmatrix} \underbrace{\begin{pmatrix} g'^2 & -gg' \\ -gg' & g^2 \end{pmatrix}}_{\mathcal{M}} \begin{pmatrix} B_{\mu} \\ W^3_{\mu} \end{pmatrix},$$

To create physical bosons that are linear combinations of the non-physical ones, we need to diagonalize the mass matrix $\mathcal{M}$. This process can be done by applying transformations $\mathcal{R}$ such that:

$$\begin{pmatrix} B^{\mu} & W^{3\mu} \end{pmatrix} \mathcal{R} \underbrace{\left[\mathcal{R}^{-1}\mathcal{M}\mathcal{R}\right]}_{\text{Diagonal}} \mathcal{R}^{-1} \begin{pmatrix} B_{\mu} \\ W^3_{\mu} \end{pmatrix}. \tag{1.68}$$

This type of transformation on the matrix $\mathcal{M}$ is called a similarity transformation. To find the form of the transformation $\mathcal{R}$, we need the eigenvectors of $\mathcal{M}$. Using the characteristic equation method, we find that its eigenvalues are 0 and $(g'^2 + g^2)$; these eigenvectors form the matrix $\mathcal{R}$, which is given by:

$$\mathcal{R} = \frac{1}{\sqrt{g'^2 + g^2}} \begin{pmatrix} g & -g' \\ g' & g \end{pmatrix}, \tag{1.69}$$

so that

$$\mathcal{R}^{-1}\mathcal{M}\mathcal{R} = \begin{pmatrix} 0 & 0 \\ 0 & g'^2 + g^2 \end{pmatrix}. \tag{1.70}$$

The consequence of diagonalizing the matrix $\mathcal{M}$ in this way is that the form of the states B_{μ} and W^3_{μ} must also transform under the action of $\mathcal{R}$, as can be seen in the relation (1.68). This transformation on the states can be interpreted as a rotation by the angle θ_W, known as the Weinberg angle, so that:

$$\mathcal{R}_W = \mathcal{R}^{-1} = \begin{pmatrix} cos\theta_W & sin\theta_W \\ -sin\theta_W & cos\theta_W \end{pmatrix}. \tag{1.71}$$

Thus, the new rotated states are

$$\begin{pmatrix} A_{\mu} \\ Z_{\mu} \end{pmatrix} = \mathcal{R}_W \begin{pmatrix} B_{\mu} \\ W^3_{\mu} \end{pmatrix} = \begin{pmatrix} B^{\mu}cos\theta_W + W^3_{\mu}sin\theta_W \\ -B^{\mu}sin\theta_W + W^3_{\mu}cos\theta_W \end{pmatrix}, \tag{1.72}$$

therefore, $cos\theta_W \equiv \frac{g}{\sqrt{g'^2+g^2}}$ and $sin\theta_W \equiv \frac{g'}{\sqrt{g'^2+g^2}}$. With this, we can rewrite the terms of the relation (1.72) in terms of the couplings g and g', so that [19]:

$$A_\mu = \frac{1}{\sqrt{g'^2+g^2}}(gB_\mu + g'W_\mu^3), \tag{1.73}$$

$$Z_\mu = \frac{1}{\sqrt{g'^2+g^2}}(-g'B_\mu + gW_\mu^3). \tag{1.74}$$

Furthermore, we can also rewrite the relation (1.68) in terms of the physical bosons A_μ e Z_μ, making explicit what will become the mass terms:

$$\begin{pmatrix} A^\mu & Z^\mu \end{pmatrix} \begin{pmatrix} 0 & 0 \\ 0 & g'^2+g^2 \end{pmatrix} \begin{pmatrix} A_\mu \\ Z_\mu \end{pmatrix} = (0)A_\mu A^\mu + (g'^2+g^2)Z_\mu Z^\mu. \tag{1.75}$$

Upon analysis, the boson A_μ is the photon since it has no mass term, while the other one that does have a mass term is the boson Z^μ, with both being neutral bosons in the theory. The absence of mass for the photon occurs because after the SSB, the resulting group is the $U(1)_{EM}$, and any gauge boson associated with a conserved symmetry is massless. To make explicit the mass terms for the bosons W_μ e Z_μ, we apply the definitions of the new physical fields (1.67) and (1.75) to the kinetic term of the scalar Lagrangian (1.66), finding that:

$$\begin{aligned} \mathcal{L}_{Scalar} \supset \frac{1}{2}\partial_\mu h \partial^\mu h + \frac{(v+h)^2}{4}g^2 W_\mu^+ W^{-\mu} \\ + \frac{(v+h)^2}{8}\left[(0)A_\mu A^\mu + (g'^2+g^2)Z_\mu Z^\mu\right], \end{aligned} \tag{1.76}$$

$$\mathcal{L}_{Scalar} \supset \frac{1}{2}\partial_\mu h \partial^\mu h + M_W^2 W_\mu^+ W^{-\mu} + \frac{1}{2}M_Z^2 Z_\mu Z^\mu + ... \tag{1.77}$$

therefore[10]

$$M_W^2 = \frac{g^2 v^2}{4} \quad ; \quad M_Z^2 = \frac{v^2}{4}(g'^2+g^2) \quad ; \quad M_A^2 = 0. \tag{1.78}$$

Here, we will focus on the mass of the electroweak gauge bosons, but the Lagrangian (1.76) also presents interaction terms between these gauge bosons and the Higgs. These interactions will be discussed in the next subsection (1.5.2). One thing we can observe is that the mass of the boson Z_μ is related to that of the boson W_μ. Writing this relation in terms of the Weinberg angle θ_W, we have:

[10] The reason why the mass term of Z_μ has a factor of 1/2 is because it is a real field (1.74), unlike W_μ which is a complex field (1.67).

$$M_Z^2 = \frac{g^2 v^2}{4cos^2\theta_W} = \frac{M_W^2}{c_W^2}. \tag{1.79}$$

From now on, we can relate the expressions for the gauge boson masses with experimental data to find their exact values. Later, when we deal with the charged current for leptons, we will be able to use it to describe beta decay, thus relating the electroweak theory presented here with Fermi's effective theory. Doing so will provide us with a relation between the weak coupling constant g, the mass of the boson W_μ, and Fermi's constant G_F:

$$\frac{g}{2\sqrt{2}} = \left(\frac{M_W^2 G_F}{\sqrt{2}}\right)^{1/2}. \tag{1.80}$$

Therefore, we can relate this expression to the mass of the boson W_μ in (1.78), and find the value for the VEV:

$$v = (\sqrt{2}G_F)^{1/2} \approx 246\,\text{GeV}. \tag{1.81}$$

In addition to the presented relations, another very important one is the relation that connects the couplings g and g' with the electric charge e through the Weinberg angle θ_W:

$$e = g s_W = g' c_W. \tag{1.82}$$

Since Fermi's constant G_F and the electric charge e have well-defined values, if we find the values for c_W and s_W, we can determine the masses of the bosons W_μ and Z_μ. From processes involving Forward-Backward Asymmetry [20], it is possible to find the value of s_W as $s_W^2 \approx 0.2314 \pm 0.00012$, thus allowing us to determine the masses of the gauge bosons which is given by:

$$M_W^2 = \frac{e^2 v^2}{4 s_W^2} \approx (78\,\text{GeV})^2,$$
$$M_Z^2 = \frac{e^2 v^2}{4 s_W^2 c_W^2} \approx (89\,\text{GeV})^2.$$

The updated values for the masses of these bosons are given by [21]:

$$M_W = 80.377 \pm 0.012\,\text{GeV} \quad ; \quad M_Z = 91.1876 \pm 0.0021\,\text{GeV}. \tag{1.83}$$

1.5.2 Electroweak gauge bosons interactions with de Higgs

Now we can discuss the other terms that arise from the kinetic part of the scalar sector Lagrangian. Consider the terms involving only the boson W_μ in the Lagrangian (1.76):

$$\frac{(v+h)^2}{4}g^2 W_\mu^+ W^{-\mu} = \frac{1}{4}g^2 v^2 W_\mu^+ W^{-\mu} + \frac{1}{2}g^2 v W_\mu^+ W^{-\mu} h + \frac{1}{4}g^2 W_\mu^+ W^{-\mu} hh \tag{1.84}$$

The first is the mass term, while the others are triple and quartic interaction terms between the boson W_μ and the Higgs. As shown previously, $M_W^2 = g^2 v^2/4$, the coupling strength of the $W_\mu W^\mu h$ and $W_\mu W^\mu hh$ vertices are given by [22]:

$$g_{hWW} = \frac{1}{2}g^2 v \equiv g M_W \qquad ; \qquad g_{hhWW} = \frac{q^2}{4} \equiv \frac{M_W^2}{v^2}. \tag{1.85}$$

This means that we can rewrite the interaction terms with the Higgs such that the coupling of the interactions is proportional to the mass of W_μ. The same applies to the couplings of the interactions between Z_μ and the Higgs:

$$\begin{aligned}\frac{(v+h)^2}{8}(g'^2+g^2)Z_\mu Z^\mu = \frac{1}{2}\frac{(g'^2+g^2)}{4}v^2 Z_\mu Z^\mu + \frac{1}{2}\frac{(g'^2+g^2)}{4}v Z_\mu Z^\mu h \\ + \frac{1}{2}\frac{(g'^2+g^2)}{4}Z_\mu Z^\mu hh,\end{aligned} \tag{1.86}$$

as $M_Z^2 = \frac{v^2}{4}(g'^2+g^2)$, the coupling strengths of the interaction terms are:

$$g_{hZZ} \equiv \frac{M_Z^2}{2v} \qquad ; \qquad g_{hhZZ} \equiv \frac{M_Z^2}{2v^2}. \tag{1.87}$$

This property of the Higgs interacting with gauge bosons through a coupling that depends on the mass of the boson also applies to fermions, so that the coupling between the Higgs and the fermions is of the form $g_{hf\bar{f}} = M_f/v$. The way this coupling is derived will be shown in the section on the Yukawa sector (1.7).

1.5.3 Higgs boson mass

We have extracted the mass terms of the gauge bosons and their interactions with the Higgs from the kinetic term of the scalar sector thus far. We will explore the potential term and find a mass term for the Higgs boson. Expanding the potential term of the scalar sector Lagrangian (1.64), we find that:

$$\mathcal{L}_{Scalar} \supset -\mu^2\frac{(v+h)^2}{2} - \lambda\frac{(v+h)^4}{4}. \tag{1.88}$$

We will consider only the terms with h^2, which will give the mass term; the others are self-interaction terms of the Higgs. Additionally, we will use the relation $v^2 = -\mu^2/\lambda$, so that:

$$\begin{aligned}\mathcal{L}_{Scalar} \supset & -\frac{\mu^2}{2}h^2 - \lambda v^2 h^2 - \frac{\lambda}{2}v^2 h^2 + ... \\ = & -\frac{1}{2}(-2\mu^2 h^2) + ...\end{aligned}$$

so that the mass of the Higgs boson is given by:

$$M_h = \sqrt{-2\mu^2} = \sqrt{2\lambda} = \left(\frac{\sqrt{2}}{G_F}\right)^{1/2}\sqrt{\lambda}. \tag{1.89}$$

Among the parameters that define the Higgs mass, Fermi's constant G_F has a known value, but the only requirement the model imposes on the parameter λ is that it must be positive. Thus, to precisely determine the mass of the Higgs boson, it is necessary to study its interaction with other SM particles as well as its self-interactions. As the Higgs couples to particles proportional their masses, the channel used for the discovery of the Higgs in the ATLAS detector at CERN was the "golden channel" [23], a channel that arises from proton-proton collisions which, through a top quark loop, generates ($h \to ZZ^* \to 4l$), where $4l$ represents the four leptons in the final state. The most up-to-date value for the Higgs mass is given by [21]:

$$M_h = 125.18 \pm 0.16 \text{ GeV}. \tag{1.90}$$

1.6 Gauge bosons sector

It is good timing to understand how these bosonic fields have their dynamics described in the SM, as well as how they interact with each other. As seen previously, to describe these fields, we use the kinetic term of the Proca Lagrangian (1.13), and for interaction terms between them to exist, we must consider a non-Abelian gauge theory, as discussed in subsection (1.2.1). Since the electroweak theory before SSB obeys the $SU(2)_L \times U(1)_Y$ symmetry, the gauge bosons sector Lagrangian takes the form:

$$\mathcal{L}_{Gauge} = -\frac{1}{4}B_{\mu\nu}B^{\mu\nu} - \frac{1}{4}W^a_{\mu\nu}W^{\mu\nu}_a, \tag{1.91}$$

where $W^a_{\mu\nu}$ and $B_{\mu\nu}$ are the field-strength tensors described in (1.55), which are associated with the bosons W^a_μ and B_μ, respectively. Expanding the last term of (1.91), we find that:

$$
\begin{aligned}
-\frac{1}{4}W^a_{\mu\nu}W^{\mu\nu}_a = &-\frac{1}{2}\left[(\partial_\nu W^a_\mu)(\partial^\nu W^\mu_a) - (\partial_\nu W^a_\mu)(\partial^\mu W^\nu_a)\right] \\
&- g\epsilon^{abc}(\partial^\nu W^\mu_a)(W_{b\mu}W_{c\nu}) \\
&- \frac{g^2}{4}(W_{b\mu}W_{c\nu})(W^{b\mu}W^{c\nu} - W^{c\mu}W^{b\nu}).
\end{aligned} \tag{1.92}
$$

The term $-\frac{1}{4}B_{\mu\nu}B^{\mu\nu}$ is similar but without the cubic and quartic interaction terms:

$$
-\frac{1}{4}B_{\mu\nu}B^{\mu\nu} = -\frac{1}{2}\left[(\partial_\nu B_\mu)(\partial^\nu B^\mu) - (\partial_\nu B_\mu)(\partial^\mu B^\nu)\right]. \tag{1.93}
$$

Since these fields are non-physical, it is necessary to rewrite them in terms of the physical ones, considering (1.67), (1.73), and (1.74):

$$
\begin{aligned}
&W^1_\mu = \frac{W^+_\mu + W^-_\mu}{\sqrt{2}} \quad ; \quad W^2_\mu = \frac{i(W^+_\mu - W^-_\mu)}{\sqrt{2}} \quad ; \quad W^3_\mu = A_\mu s_W + Z_\mu c_W \quad ; \\
&B_\mu = A_\mu c_W - Z_\mu s_W.
\end{aligned} \tag{1.94}
$$

Applying (1.94) in to (1.92) and (1.93) and expanding only the cubic interaction terms $\mathcal{L}_3$ and quartic terms $\mathcal{L}_4$, we find that [24]:

$$
\begin{aligned}
\mathcal{L}_3 = &\, ie\cot_W\left[(\partial^\mu W^{-\nu} - \partial^\nu W^{-\mu})W^+_\mu Z_\nu - (\partial^\mu W^{+\nu} - \partial^\nu W^{+\mu})W^-_\mu Z_\nu + W^-_\mu W^+_\nu(\partial^\mu Z^\nu - \partial^\nu Z^\mu)\right] \\
&+ ie\left[(\partial^\mu W^{-\nu} - \partial^\nu W^{-\mu})W^+_\mu A_\nu - (\partial^\mu W^{+\nu} - \partial^\mu W^{+\nu})W^-_\mu A_\nu + W^-_\mu W^+_\mu(\partial^\mu A^\nu - \partial^\nu A^\mu)\right];
\end{aligned} \tag{1.95}
$$

$$
\begin{aligned}
\mathcal{L}_4 = &-\frac{e^2}{2s^2_W}\left[(W^+_\mu W^{-\mu})^2 - W^+_\mu W^{+\mu}W^-_\nu W^{-\nu}\right] - e^2 cot^2_W\left[W^+_\mu W^{-\mu}Z_\nu Z^\nu - W^+_\mu Z^\mu W^-_\nu Z^\nu\right] \\
&- e^2 cot_W\left[2W^+_\mu W^{-\mu}Z_\nu A^\nu - W^+_\mu Z^\mu W^-_\nu A^\nu - W^+_\mu A^\mu W^-_\nu Z^\nu\right] \\
&- e^2\left[W^+_\mu W^\mu A_\nu A^\nu - W^+_\mu A^\mu W^-_\nu A^\nu\right].
\end{aligned} \tag{1.96}
$$

These are the vertices of the interactions between $W^\pm_\mu$, Z_μ, and A_μ. Note that all the terms involve combinations of W^+W^-, since the total electric charge of the Lagrangian must be zero. Furthermore, since the photon only interacts with charged particles, there is no interaction term between just the photon A_μ and the boson Z_μ.

1.7 Yukawa sector

When we introduced the fermionic field (spinors), it was shown that in the SM these particles can be written in terms of their left-handed and right-handed components, with each of these components being treated differently. While the left-handed components are written in the form of a doublet, the right-handed ones are in the form of a singlet. This occurs precisely because of the $SU(2)_L$ symmetry, which is associated with fermions through only one of their chiralities. As a result, initially, mass terms for fermions cannot be created, since the fermionic field ψ needs to have both left-handed ψ_L and right-handed ψ_R components in the form of doublets:

$$M\bar{\psi}\psi = M\left[\bar{\psi}_R\psi_L + \bar{\psi}_L\psi_R\right]. \tag{1.97}$$

Therefore, to give mass to fermions without violating the $SU(2)_L$ gauge symmetry, the Yukawa Lagrangian was introduced. This Lagrangian incorporates the Higgs doublet ϕ into a mass term of the type (1.97), requiring only the inclusion of a constant G_Y called the Yukawa constant, so that:

$$\mathcal{L}_{Yukawa} = -G_Y\left[\bar{\psi}_R(\phi^\dagger\psi_L) + (\bar{\psi}_L\phi)\psi_R\right].$$

With the introduction of the Higgs doublet, this mass term remains invariant under gauge transformations, since ϕ is associated with the $SU(2)_L$ symmetry and therefore has isospin, in addition to having hypercharge $Y = -1$. Regarding the Yukawa constant, it initially does not have a defined value, but it can be inferred from the masses of the fermions themselves.

1.7.1 The charged leptons masses

Since neutrinos are massless particles in the SM, as they do not have a right-handed component, only the charged leptons have mass terms. Considering the definition (1.57), the Yukawa Lagrangian for the charged leptons of generation l is given by:

$$\mathcal{L}^l_{Yukawa} = -G_l\left[\bar{R}_l(\phi^\dagger L_l) + (\bar{L}_l\phi)R_l\right]. \tag{1.98}$$

Expanding the doublet L_l, the singlet R_l, and the Higgs doublet ϕ, we find that:

$$\begin{aligned}\mathcal{L}^l_{Yukawa} &= -G_l\left[\bar{l}_R\begin{pmatrix}0 & \frac{v+h}{\sqrt{2}}\end{pmatrix}\begin{pmatrix}\nu_{lL}\\ l_L\end{pmatrix} + \begin{pmatrix}\bar{\nu}_{lL} & \bar{l}_L\end{pmatrix}\begin{pmatrix}0\\ \frac{v+h}{\sqrt{2}}\end{pmatrix} l_R\right]\\ &= -G_l\frac{(v+h)}{\sqrt{2}}\left[\bar{l}_R l_L + \bar{l}_L l_R\right],\end{aligned} \tag{1.99}$$

as $\bar{l}l = \bar{l}_R l_L + \bar{l}_L l_R$, then

$$\mathcal{L}^{l}_{Yukawa} = -\frac{G_l v}{\sqrt{2}}\bar{l}l - \frac{G_l}{\sqrt{2}}\bar{l}lh. \tag{1.100}$$

Therefore, the mass of the charged lepton of generation l is given by:

$$M_l = -\frac{G_l v}{\sqrt{2}}. \tag{1.101}$$

Moreover, the charged leptons interact with the Higgs boson proportionally to their mass, just like the gauge bosons:

$$g_{h\bar{l}l} = \frac{M_l}{v}. \tag{1.102}$$

It is worth noting that although neutrinos are massless in the SM, there is currently strong evidence supporting the existence of mass for them. This is due to the observation of neutrino oscillations, that is, the ability of neutrinos to oscillate between their lepton flavors. This observed oscillation implies that at least two of the SM neutrinos must have nonzero mass. The first evidence of this oscillation phenomenon came from the observation of muon neutrinos originating from the atmosphere through the Super-Kamiokande detector [25], and from the observation of electron neutrinos originating from the Sun at Canada's Sudbury Neutrino Observatory [26].

1.7.2 The quarks masses

The procedure for generating mass for the quarks is similar to the one used previously for the charged leptons. However, unlike the leptons, all quarks are massive. Therefore, it is necessary to give mass to both components of the $SU(2)_L$ doublet. For this, we need to define the conjugate Higgs doublet $\tilde{\phi}$, given by:

$$\tilde{\phi} = i\sigma_2\phi^* = \begin{pmatrix} \phi^{0^*} \\ -\phi^- \end{pmatrix} \tag{1.103}$$

This doublet is the representation of an invariant transformation under $SU(2)_L$ of the original doublet, having the same properties as the Higgs doublet. The differences are that this conjugate doublet has hypercharge $Y = -1$, and the component that develops a VEV is the one with isospin $T^3 = +1/2$, unlike the original Higgs doublet where the component that develops a VEV is the one with isospin $T^3 = -1/2$. It is precisely this characteristic that allows this doublet to give mass to the up-like quarks. Therefore, considering the notation (1.58), the Yukawa Lagrangian for the quarks is written as [14]:

$$\mathcal{L}^{q}_{Yukawa} = -\sum_{i,j=1}^{3}\left[G^{U}_{ij}\bar{R}_{U_i}\left(\tilde{\phi}^{\dagger}L_j\right) + G^{D}_{ij}\bar{R}_{D_i}\left(\phi^{\dagger}L_j\right)\right] + \text{h.c}, \tag{1.104}$$

where $U_i = u, c, t$ are the up-like quarks, and $D_i = d, s, b$ are the down-like quarks. After the SSB, the doublets take the form:

$$\phi = \frac{(v+h)}{\sqrt{2}}\begin{pmatrix}0\\1\end{pmatrix} \quad ; \quad \tilde{\phi} = \frac{(v+h)}{\sqrt{2}}\begin{pmatrix}1\\0\end{pmatrix}. \tag{1.105}$$

Applying them in (1.104), we find:

$$\begin{aligned}\mathcal{L}^{q}_{Yukawa} &= -\frac{(v+h)}{\sqrt{2}}\sum_{i,j=1}^{3}\left[G^{U}_{ij}\bar{R}_{U_i}\begin{pmatrix}1 & 0\end{pmatrix}\begin{pmatrix}U_{jL}\\D_{jL}\end{pmatrix} + G^{D}_{ij}\bar{R}_{D_i}\begin{pmatrix}0 & 1\end{pmatrix}\begin{pmatrix}U_{jL}\\D_{jL}\end{pmatrix}\right] + \text{h.c}\\ &= -\frac{(v+h)}{\sqrt{2}}\sum_{i,j=1}^{3}\left[G^{U}_{ij}(\bar{U}_{iR}U_{jL}) + G^{D}_{ij}(\bar{D}_{iR}D_{jL})\right] + \text{h.c}\end{aligned} \tag{1.106}$$

Therefore, the mass matrix for the quarks is given by $M^{U(D)}_{ij} = (v/\sqrt{2})G^{U(D)}_{ij}$. However, this matrix is not diagonal, so the quarks presented above do not form a mass eigenstate. Thus, we consider the change in notation: $U_i \to U'_i$, $D_i \to D'_i$. It is possible to rewrite the mass terms of equation (1.106) in terms of a product of matrices:

$$-\begin{pmatrix}\bar{u}' & \bar{c}' & \bar{t}'\end{pmatrix}_R \mathcal{M}^{U}\begin{pmatrix}u'\\c'\\t'\end{pmatrix}_L - \begin{pmatrix}\bar{d}' & \bar{s}' & \bar{b}'\end{pmatrix}_R \mathcal{M}^{D}\begin{pmatrix}d'\\s'\\b'\end{pmatrix}_L + \text{h.c.} \tag{1.107}$$

To diagonalize the mass matrix $M^{U(D)}_{ij}$, we can use the same method presented in subsection (1.5.1), so that:

$$\begin{aligned}&-\begin{pmatrix}\bar{u}' & \bar{c}' & \bar{t}'\end{pmatrix}_R U_R\left(U_R^{-1}\mathcal{M}^{U}U_L\right)U_L^{-1}\begin{pmatrix}u'\\c'\\t'\end{pmatrix}_L\\ &-\begin{pmatrix}\bar{d}' & \bar{s}' & \bar{b}'\end{pmatrix}_R D_R\left(D_R^{-1}\mathcal{M}^{D}D_L\right)D_L^{-1}\begin{pmatrix}d'\\s'\\b'\end{pmatrix}_L + \text{h.c.}\end{aligned} \tag{1.108}$$

Thus, the mass matrices for the up-like and down-like quarks are given by:

$$U_R^{-1}\mathcal{M}^U U_L = \begin{pmatrix} M_u & 0 & 0 \\ 0 & M_c & 0 \\ 0 & 0 & M_t \end{pmatrix} \quad ; \quad D_R^{-1}\mathcal{M}^D D_L = \begin{pmatrix} M_d & 0 & 0 \\ 0 & M_s & 0 \\ 0 & 0 & M_b \end{pmatrix} \tag{1.109}$$

And the mass eigenstates, which are linear superpositions of the weak eigenstates, are given by the unitary transformations:

$$\begin{pmatrix} u \\ c \\ t \end{pmatrix}_{L,R} = U_{L,R}^{-1} \begin{pmatrix} u' \\ c' \\ t' \end{pmatrix}_{L,R} \quad ; \quad \begin{pmatrix} d \\ s \\ b \end{pmatrix}_{L,R} = D_{L,R}^{-1} \begin{pmatrix} d' \\ s' \\ b' \end{pmatrix}_{L,R} \tag{1.110}$$

In addition to the mass terms, equation (1.106) also presents the interaction terms between the quarks q and the Higgs boson h. As in other cases, the strength of these couplings is proportional to the mass of the quarks:

$$g_{h\bar{q}q} = \frac{M_q}{v} \tag{1.111}$$

1.8 Fermions sector

This sector of the electroweak Lagrangian is responsible for generating the interactions between fermions and gauge bosons, that is, the interaction between the matter content of the model and its mediating bosons. As described earlier, these interaction terms arise from the kinetic term of the Dirac Lagrangian when we impose local gauge invariance on it, through the choice of an appropriate invariant covariant derivative D_μ. Therefore, if the fermionic field is ψ, the Lagrangian for the Fermions sector is given by:

$$\mathcal{L}_{Fermions} = i\bar{\psi}\gamma^\mu D_\mu \psi. \tag{1.112}$$

It has been discussed several times that the weak interaction violates parity, and because of this, the Lagrangian must have a (V-A) structure, which specifies the chiral component of the fermions that is part of the interaction. This characteristic is the reason why the symmetry group of the electroweak model is $SU(2)_L \times U(1)_Y$, where the left-handed chirality is made explicit. Such a choice influences the form of the invariant covariant derivative (1.56), which acts differently on the left-handed and right-handed chiralities of a given fermion, therefore:

$$\mathcal{L}_{Fermions} = i\bar{\psi}_L\gamma^\mu \left(\partial_\mu - ig\frac{\tau^a}{2}W_\mu^a - ig'\frac{Y}{2}B_\mu\right)\psi_L + i\bar{\psi}_R\gamma^\mu \left(\partial_\mu - ig'\frac{Y}{2}B_\mu\right)\psi_R. \tag{1.113}$$

As discussed earlier in subsection (1.5.1), the bosons W_μ^a and B_μ are not physical, and it is necessary to rewrite them in the mass eigenstate basis: $W_\mu^\pm$, Z_μ. If we do this in the Lagrangian (1.113), the interactions will be divided into two parts: a **charged current** mediated by the boson $W_\mu^\pm$, which involves only left-handed fermions; and a **neutral current** mediated by the bosons Z_μ and A_μ, which involves both chiral components of the fermions.

1.8.1 The Charged Current

The charged current is found from the off-diagonal terms of the Lagrangian (1.113), so that the physical bosons $W_\mu^\pm$ will interact only with the left-handed fermions arranged in doublets. Moreover, this current is responsible for beta decay. For all generations of leptons, the charged current is given by:

$$\mathcal{L}_{Leptons}^{cc} = -\frac{g}{\sqrt{2}} \sum_l \bar{L}_l \gamma^\mu \begin{pmatrix} 0 & W_\mu^+ \\ W_\mu^- & 0 \end{pmatrix} L_l, \tag{1.114}$$

where l represents each generation of leptons $l = e, \mu, \nu$. Expanding the doublets according to the definition (1.57), we find that:

$$\mathcal{L}_{Leptons}^{cc} = -\frac{g}{2\sqrt{2}} \sum_l \left[\bar{\nu}_l \gamma^\mu (1-\gamma^5) l W_\mu^+ + \bar{l} \gamma^\mu (1-\gamma^5) \nu_l W_\mu^- \right], \tag{1.115}$$

reproducing exactly the (V-A) structure of the weak charged current. Moreover, it is important to note that the charged current interaction for leptons occurs between leptons of the same generation ($\bar{\nu}_e e$, $\bar{\nu}_\mu \mu$, and $\bar{\nu}_\tau \tau$), thus conserving lepton flavor.

For quarks, however, the charged current is slightly different. In addition to involving quarks of the same generation ($\bar{u}d$, $\bar{c}s$, and $\bar{t}b$), it also involves quarks from different generations (e.g. $\bar{u}s$, $\bar{c}d$), meaning that it does not conserve quark flavor. By convention, this transition between different generations in the interaction occurs between the down-like quarks. The description of this phenomenon originated in 1963 from N. Cabibbo's study of what is now known as the decay probability of down and strange quarks into up quarks [27]. To describe such transitions, the Cabibbo angle θ_C is used, which mixes the mass eigenstates (d, s) to generate the interaction eigenstates (d', s') that are effectively part of the charged current. It is worth mentioning that interactions between quarks of different generations are suppressed compared to interactions between quarks of the same generation, and this characteristic is incorporated in the value of the Cabibbo angle. That said, the relation between mass and interaction states is given by the Cabibbo matrix:

$$\begin{pmatrix} d' \\ s' \end{pmatrix} = \begin{pmatrix} cos\theta_C & sin\theta_C \\ -sin\theta_C & cos\theta_C \end{pmatrix} \begin{pmatrix} d \\ s \end{pmatrix}. \tag{1.116}$$

For historical reasons, this matrix relates only the states of the down-like quarks of the 1^{st} and 2^{nd} generations. However, later, the 3^{rd} generation was added to the mix, thus generating the Cabibbo-Kobayashi-Maskawa (CKM) matrix:

$$\begin{pmatrix} d' \\ s' \\ b' \end{pmatrix} = V_{CKM} \begin{pmatrix} d \\ s \\ b \end{pmatrix}, \tag{1.117}$$

where V_{CKM} is a 3×3 unitary matrix given by:

$$V_{CKM} = \begin{pmatrix} c_{12}c_{13} & s_{12}c_{13} & s_{13}e^{-i\delta_{13}} \\ -s_{12}c_{23} - c_{12}s_{23}s_{13}e^{i\delta_{13}} & c_{12}c_{23} - s_{12}s_{23}s_{13}e^{i\delta_{13}} & s_{23}c_{13} \\ s_{12}s_{23} - c_{12}c_{23}s_{13}e^{i\delta_{13}} & -c_{12}s_{23} - s_{12}c_{23}s_{13}e^{i\delta_{13}} & c_{23}c_{13} \end{pmatrix}. \tag{1.118}$$

The abbreviation $cos\theta_{ij} = c_{ij}$ was used above, where θ_{ij} represents the mixing angle between generations i and j, while the term δ_{13} is a phase. It can be observed that if we consider the three generations of quarks, it is not always possible for the V_{CKM} matrix to be real, that is, $\delta_{13} = 0$, and therefore the weak interaction can violate the CP symmetry. [11] If we consider that the transition to the 3^{rd} generation is completely suppressed ($\theta_{13} = \theta_{23} \to 0$), the CKM matrix is reduced to the Cabibbo matrix, where $\theta_{12} \to \theta_C$, so that:

$$V_{CKM} \to \begin{pmatrix} c_{12} & s_{12} & 0 \\ -s_{12} & c_{12} & 0 \\ 0 & 0 & 1 \end{pmatrix}. \tag{1.119}$$

It is possible to construct the charged current using the definition of the mass eigenstates in terms of the weak eigenstates (1.110), so that it is given by:

$$\mathcal{L}^{cc}_{Quarks} = -\frac{g}{2\sqrt{2}} \begin{pmatrix} \bar{u} & \bar{c} & \bar{t} \end{pmatrix}_L \gamma^\mu (U_L^+ D_L) \begin{pmatrix} d \\ s \\ b \end{pmatrix}_L W^+_\mu + \text{h.c.} \tag{1.120}$$

If we consider that the CKM matrix is given by $V_{CKM} = U_L^+ D_L$, in addition to finding interaction terms between physical particles (in the mass eigenstate), interaction terms between quarks of different generations will also arise. Therefore, considering the relation (1.117), the Lagrangian becomes:

$$\mathcal{L}^{cc}_{Quarks} = -\frac{g}{2\sqrt{2}} \left[\bar{u}\gamma^\mu(1-\gamma^5)d' + \bar{c}\gamma^\mu(1-\gamma^5)s' + \bar{t}\gamma^\mu(1-\gamma^5)b' \right] W^+_\mu + \text{h.c.} \tag{1.121}$$

[11] The conjugate charge symmetry C reverses the particle charge, while parity symmetry P exchanges left-handed and right-handed states.

By applying unitarity constraints and assuming the existence of only three generations, the experimental values for the elements of the CKM matrix can be derived from weak quark decays and deep inelastic neutrino scattering; therefore, according to the Particle Data Group (PDG), the magnitudes of all nine CKM elements obtained from experiments are [21]:

$$|V_{CKM}| = \begin{pmatrix} 0.97435 \pm 0.00016 & 0.22500 \pm 0.00067 & 0.00369 \pm 0.00011 \\ 0.22486 \pm 0.00067 & 0.97349 \pm 0.00016 & 0.04182^{+0.00085}_{-0.00074} \\ 0.00857^{+0.00020}_{-0.00018} & 0.04110^{+0.00083}_{-0.00072} & 0.999118^{+0.000031}_{-0.000036} \end{pmatrix}. \quad (1.122)$$

Note that the further from the diagonal, the smaller the magnitude of the coupling becomes, favoring interactions between quarks of the same generation, as discussed earlier. To better illustrate how the charged weak interaction allows quarks to decay into other generations, consider the diagram below:

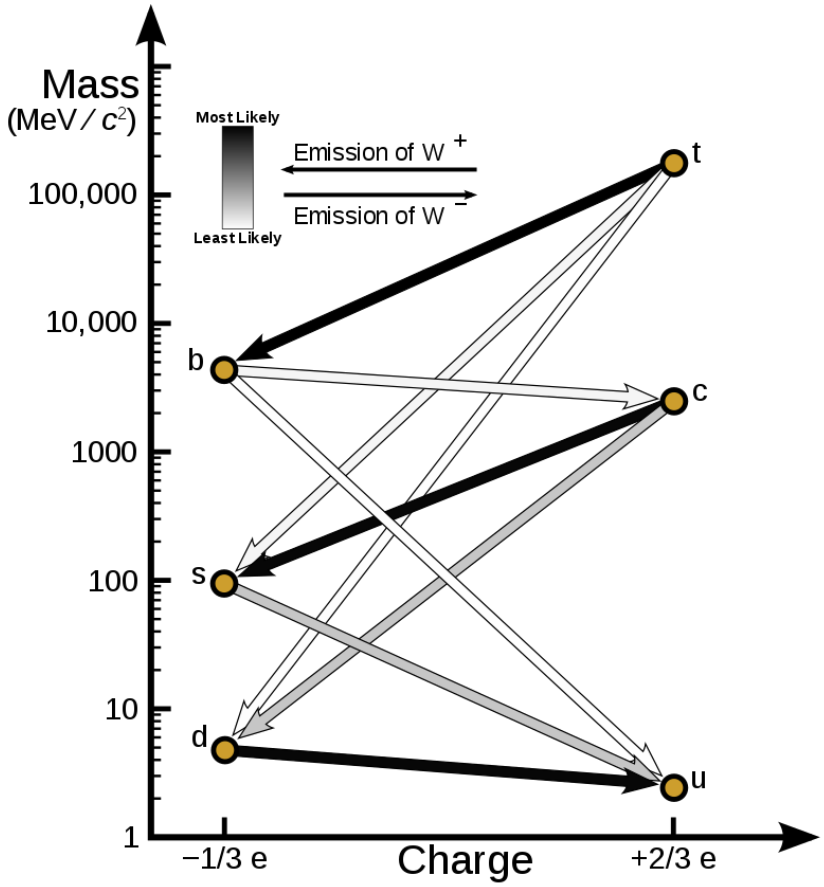

Figure 2 – A diagram illustrating the decay pathways resulting from the charged weak interaction, along with an indication of their probabilities. The thickness of the lines corresponds to the CKM parameters [28].

1.8.2 The Neutral Current

The neutral current represents interactions between fermions mediated by the neutral bosons Z_μ and A_μ. Historically, the electroweak theory predicted the existence of a charged boson $W_\mu^\pm$ to explain beta decay, and along with it, the existence of the Z_μ boson was also predicted, although it had not yet been observed [7]. Since the Z_μ boson behaves similarly to the photon A_μ, its contribution to the process is more significant only when it is created in collisions at energies near its mass ($M_Z \sim 91GeV$), i.e., at its resonance. Therefore, the observation of neutral current interactions involving particles other than neutrinos required significant investments in particle accelerators and detectors. This type of interaction was observed for the first time only in 1973 in the huge Gargamelle bubble chamber [29]. However, the discovery of the $W_\mu^\pm$ and Z_μ bosons themselves only occurred in 1983 through the Super Proton Synchrotron, where experiments led by Carlo Rubbia and Simon van der Meer (UA1 and UA2) detected $W_\mu^\pm$ bosons in January, followed by the Z_μ boson in May of the same year [30, 31].

From the diagonal terms of the fermion Lagrangian (1.113), it is possible to find the neutral current. However, the bosons made explicit in this Lagrangian are not the physical bosons, requiring the use of relations (1.94). Therefore, for leptons, the neutral current is given by:

$$\mathcal{L}^{nc}_{Leptons} = -gs_W \sum_l \bar{l}\gamma^\mu l A_\mu - \frac{g}{2c_W}\sum_l \left[\bar{\nu}_l(g_V^\nu - g_A^\nu\gamma^5)\nu_l + \bar{l}(g_V^l - g_A^l\gamma^5)l\right] Z_\mu, \quad (1.123)$$

so that $g_V = T^3 - 2Qs_W^2$ and $g_A = T^3$, where Q is the electric charge operator and T^3 is the weak isospin. As can be seen, there are no interaction terms between the photon A_μ and the neutrino, as it does not have an electric charge; furthermore, according to QED, the coupling of the interaction with the photon depends on the electric charge e, so from (1.123) it is possible to find the relation: $e = gs_W = g'c_W$, which was previously used in (1.82). Finally, for quarks, the neutral current is given by:

$$\mathcal{L}^{nc}_{Quarks} = -\sum_{\psi=u,\dots,b} q_\psi \bar{\psi}\gamma^\mu\psi A_\mu - \frac{g}{2c_W}\sum_{\psi=u,\dots,b}\bar{\psi}\gamma^\mu(g_V^\psi - g_A^\psi\gamma^5)\psi Z_\mu, \quad (1.124)$$

where q_ψ is the electric charge of the quark ψ. Although there is flavor violation in the charged current, there is no indication that the same should happen in the neutral current. Therefore, this possibility is not considered in the SM. We had considered that there is a mixing between the mass eigenstates and the weak eigenstates; to see how the neutral current is consistent with what was done previously, consider the usual transformations (1.110):

$$\begin{pmatrix}\bar{d} & \bar{s} & \bar{b}\end{pmatrix}_{L,R}\gamma^\mu \underbrace{(D_{L,R}^+ D_{L,R})}_{Unitary}\begin{pmatrix}d\\ s\\ b\end{pmatrix}_{L,R} = \begin{pmatrix}\bar{d} & \bar{s} & \bar{b}\end{pmatrix}_{L,R}\gamma^\mu\begin{pmatrix}d\\ s\\ b\end{pmatrix}_{L,R}, \quad (1.125)$$

the same occurs for the up-like quarks in the neutral current. Therefore, no mixing matrix arises that generates interaction terms between quarks of different generations as happens in the charged current (1.120).

In this chapter we discuss in detail the Standard Model of electroweak interactions, its theoretical bases, and the importance of gauge symmetries, and spontaneous symmetry breaking for the generation of the particles masses. We explore how scalar, vector, and fermionic fields interact within this framework, as well as the crucial role played by the Higgs mechanism in unifying the electromagnetic and weak interactions. In the next chapter, we will enter into the study of collider physics, where we will address the interaction between high-energy particles, including relevant parameters in a collider, kinematic variables and the characteristics of the detectors used in the experimental analysis of these collisions, which is one of the fundamental research areas for the search of new physics beyond the Standard Model.

2 Collider Physics

Since the early 20th century, particle accelerators have been extensively utilized in physics research, playing a crucial role in both scientific and technological advancements over the years [32]. With respect to particle colliders, the idea is to collide head-on two focused beams[1] of very energetic particles (e^+e^-, pp, ...) with equally opposite momenta, and measure the outcome with detectors that can isolate and identify the different particles produced in the colision and their properties. In the realm of particle physics, high-energy accelerators and colliders have been the primary tools for discovering new particles and testing new theories of fundamental interactions.

With this in mind, the purpose of this chapter is to introduce the phenomenology of colliders, highlighting the main aspects for calculating collisions between accelerated particles through the study of the cross section, as well as showing the main kinematic variables used and how particles are effectively detected in an experiment. In the next chapter we take advantage of this knowledge to probe a lepthopilic Z' in a future e^+e^-. In this chapter we will address hadronic and leptonic colliders, as well as the properties of the Z boson such as its production on resonance and decay width, which are relevant aspects for the next chapter.

2.1 Interaction cross section

One of the most important variable in particle physics is the cross section, which quantifies the underlying quantum mechanical probability that an interaction will occur. To exemplify what the cross section represents, consider a beam of particles of type a colliding with only one particle of type b in its rest frame, if the particles flux ϕ_a is given by the number of particles a that cross a unit of area in a unit of time, then the rate of interaction between the particles a and the particle b is given by:

$$r_b = \sigma\phi_a, \tag{2.1}$$

where σ is the interaction cross section, which has units of area. The conventional unit used for cross sections is the barn (b), where $1b = 10^{-28}m^2$. Therefore, in this case the cross section can be seen as the interaction area of the particle b, so that if a particle a enters this area it will interact. If instead of just one target particle b we consider several particles b, then it is possible to show that the cross section equivalent to the collision between the incident flux of particles a and the target particles b is given by [22]:

[1] In addition to beam-beam colliders there are the fixed targer colliders, however they have a lower center-of-mass energy in comparison.

$$\sigma = \frac{\text{number of interactions per unit time per target particle}}{\text{incident flux}}. \tag{2.2}$$

It is important to note that thinking of the cross section as an area of interaction is not entirely accurate for subatomic particles. These particles lack a defined size and do not interact through direct contact. Instead, their cross section involves phenomena such as quantum tunneling and interactions via mediator bosons, which makes determining the probability of interaction more complex.

The crossection for a specific process can be calculated using the relativistic form of Fermi's golden rule, and the Lorentz-invariant expression for the particle flux, which are discussed in the Appendices B.1 and B.2. Consider as an example a process $a + b \rightarrow 1 + 2$ so that the initial particles of types a and b collide head-on in collinear trajectories, we might consider that particles of type a have speed and volumetric number density v_a and n_a, as well as particles of type b with v_b and n_b. The rate of interaction between these flux of colliding particles is given by:

$$\Gamma_{fi} = (v_a + v_b) n_a n_b \sigma V, \tag{2.3}$$

where V is the volume where the interaction occurs, σ is the crossection of the process, and the incidences i and f refer respectively to the initial and final state of the system. To simplify the equation (2.3) we can consider the normalization of a particle by volume $n_a = n_b = 1/V$, in addition the V factor will not appear in the final result for the crossection, so so that we can consider one particle per unit volume $V = 1$. This way the crossection is:

$$\sigma = \frac{\Gamma_{fi}}{(v_a + v_b)}. \tag{2.4}$$

Applying the relativistic form of Fermi's golden rule (B.4) to the process $a + b \rightarrow 1 + 2$ we find that the total crossection for the process is given by [22, 33]:

$$\sigma = \frac{(2\pi)^{-2}}{4E_a E_b (v_a + v_b)} \int |\mathcal{M}_{fi}|^2 \delta(E_a + E_b - E_1 - E_2) \delta^3(\mathbf{p}_a + \mathbf{p}_b - \mathbf{p}_1 - \mathbf{p}_2) \frac{d^3\mathbf{p}_1}{(2\pi)^3 2E_1} \frac{d^3\mathbf{p}_2}{(2\pi)^3 2E_2}. \tag{2.5}$$

Where $\mathcal{M}$ is known as the Feynman amplitude, and can be calculated taking into account the relevant diagrams for the process and the Feyman rules. It is worth mentioning that the equation (2.5) is written in a Lorentz-invariant form, since both the integral and the Lorentz-invariant flux factor $F = 4E_a E_b (v_a + v_b)$ are Lorentz invariant [2].

[2] Although we considered the restriction of a initial flux of collinear particles, the value of the total crossection is always Lorentz invariant.

As the total crossection value is the same in any reference frame, the most convenient option is to choose the system's center of mass (CM) reference frame. It is important to point out that despite being a convenient choice it is not often the best, especially when we want to calculate the crossection of an experiment in a fixed target collider, in these cases it is better to evaluate the crossection in the laboratory reference frame since variables such as energy and momentum, that we reconstruct from the detected particles, are measured in the reference frame of the detector itself. If we are considering for example e^+e^- collisions at the LEP or pp collisions at the LHC, the situation is simpler since the laboratory frame is the same as the CM frame.

With this in mind, for the purposes of our discussion calculating the crossection in the CM frame of the process $a + b \to 1 + 2$ will be enough, since we just want to get an idea of the format of the crossection solution. In the CM frame, the moments of the initial and final state particles obey the relations $\mathbf{p}_a = -\mathbf{p}_b = \mathbf{p}_i^*$, and $\mathbf{p}_1 = -\mathbf{p}_2 = \mathbf{p}_f^*$, in addition the energy of the center of mass is given by $E_{cm} = \sqrt{s} = (E_a^* + E_b^*)$, where s is one of the Mandelstam variables that will be further discussed in the next section. Considering the relationship $v_i = p_i/E_i$, we can find the Lorentz invariant flux factor in the CM, which is given by:

$$F = 4E_a^* E_b^* (v_a^* + v_b^*) = 4p_i^* \sqrt{s}, \tag{2.6}$$

so that the crossection is reduced to

$$\sigma = \frac{(2\pi)^{-2}}{4p_i^*\sqrt{s}} \int |\mathcal{M}_{fi}|^2 \delta(\sqrt{s} - E_1 - E_2) \delta^3(\mathbf{p}_1 + \mathbf{p}_2) \frac{d^3\mathbf{p}_1}{(2\pi)^3 2E_1} \frac{d^3\mathbf{p}_2}{(2\pi)^3 2E_2}. \tag{2.7}$$

Integrating in $d^3\mathbf{p}_2$ we find what we already expected: $\mathbf{p}_1 = -\mathbf{p}_2$. Therefore, we can write the particles energies as $E_1 = \sqrt{m_1^2 + p_1^2}$ and $E_2 = \sqrt{m_2^2 + p_1^2}$, in addition we can write in spherical coordinates $d^3\mathbf{p}_1 = p_1^2 dp_1 sin\theta d\theta d\phi = p_1^2 dp_1 d\Omega$. Using the properties of the Dirac delta-function described in the Appendix B.3 we find that:

$$\sigma = \frac{1}{64\pi^2 s} \frac{p_f^*}{p_i^*} \int |\mathcal{M}_{fi}|^2 d\Omega^*. \tag{2.8}$$

In many cases we are not interested in the total crossection, but rather in the distribution of the crossection as a function of some kinematic variable such as the solid angle $d\Omega$ or the energy of the scattered particle dE, this is known as differential crossection. In the case of the equation (2.8), the differential cross section expressed in terms of the angles of one of the final-state particles is:

$$\frac{d\sigma}{d\Omega^*} = \frac{1}{64\pi^2 s} \frac{p_f^*}{p_i^*} |\mathcal{M}_{fi}|^2. \tag{2.9}$$

2.2 Mandelstam variables

The Mandelstam variables are a set of three variables s, t, and u that are described by the momentum, energies, and angles of particles involved in a scattering process. These three variables are Lorentz invariant, making them widely used in high-energy physics to describe quantities such as the cross section in a manner that is independent of the chosen reference frame. This means that instead of directly relying on the momenta $\mathbf{p}_i$ and energies E_i of the involved particles, which change depending on the reference frame, the Mandelstam variables provide a consistent and invariant description.

For a scattering process of the type $1 + 2 \rightarrow 3 + 4$ in the CM reference frame, where the initial two particles have four-momenta p_1 and p_2, and the final two have p_3 and p_4, the Mandelstam variables are defined as [34]:

$$\begin{aligned} s =& (p_1 + p_2)^2 = (p_3 + p_4)^2 = E_{cm}^2, \\ t =& (p_1 - p_3)^2 = (p_2 - p_4)^2 = m_1^2 + m_3^2 - 2(E_1 E_3 - |\mathbf{p}_1||\mathbf{p}_3| cos\theta_{13}), \\ u =& (p_1 - p_4)^2 = (p_2 - p_3)^2 = m_1^2 + m_4^2 - 2(E_1 E_4 - |\mathbf{p}_1||\mathbf{p}_4| cos\theta_{14}). \end{aligned} \tag{2.10}$$

The variable s represents the energy of the center of mass squared E_{cm}^2, and is therefore generally used to describe the energy available for the production of new particles in a scattering. It is associated with the s-channel, as seen in Figure 3, where depending on the value of $\sqrt{s}$ the interaction can be thought of as the creation of an intermediate state (resonance) that later decays into final particles. The variables t and u represents the momentum transferred between the initial and final states, as well as the scattering angle of the particles. The difference between these two variables is in the inversion of the final state particles as seen in the following Figure.

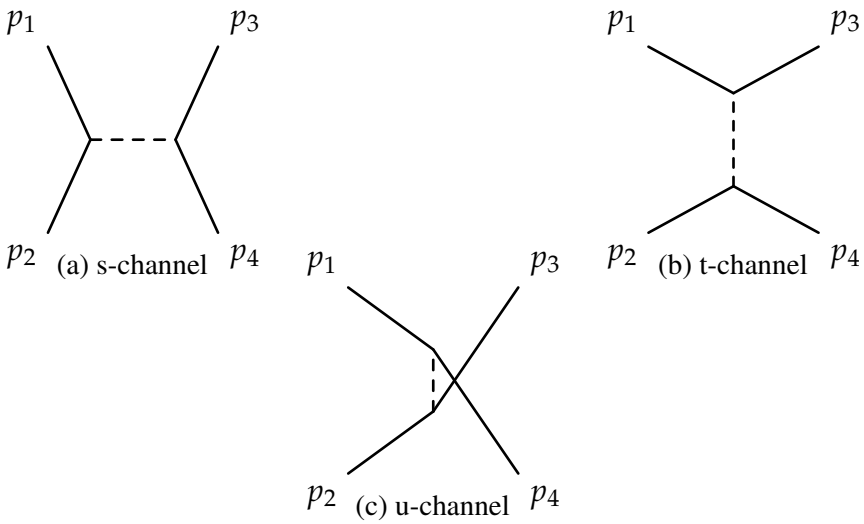

Figure 3 – Feynman diagrams of the respective Mandelstam variables.

The relationship between the three Mandelstam variables is described by: $s+t+u=\sum m_i$; where m_i are the masses of the particles involved in the scattering (initial and final state particles). Furthermore, when calculating the amplitude for the $1+2 \rightarrow 3+4$ process, the result is always a function of the scalar products between the moments of the particles in the outer legs of the diagram, so that it is possible to rewrite these scalar products in terms of the Mandelstam variables [35]:

$$\begin{aligned}
\mathbf{p}_1 \cdot \mathbf{p}_2 &= \frac{1}{2}(s - m_1^2 - m_2^2), \\
\mathbf{p}_1 \cdot \mathbf{p}_3 &= \frac{1}{2}(m_1^2 + m_3^2 - t), \\
\mathbf{p}_1 \cdot \mathbf{p}_4 &= \frac{1}{2}(m_1^2 + m_4^2 - u).
\end{aligned} \tag{2.11}$$

2.3 Collider parameters

As previously mentioned, it is possible to collide ultra-relativistic particles in two ways, head-on beams collisions and fixed target collisions. For the collision of two particles with four-momenta p_1 and p_2, in the CM reference frame $\mathbf{p}_1 + \mathbf{p}_2 = 0$ (if $m_1 = m_2$, then $E_1 = E_2 = E_{beam}$), and in the fixed target reference frame $\mathbf{p}_2 = 0$ ($E_1 = E_{beam}$), in both cases as we are considering high energy collisions the momentum and therefore the energy of the accelerated particles are typically much larger than their masses[3]. The mandelstam variable s for the two particle system is:

$$\begin{aligned}
s = (p_1 + p_2)^2 &= (E_1 + E_2)^2 - (\mathbf{p}_1 + \mathbf{p}_2)^2 \\
&= p_1^2 + p_2^2 + 2(E_1 E_2 - \mathbf{p}_1 \cdot \mathbf{p}_2).
\end{aligned} \tag{2.12}$$

For each type of experiment we can compare the value of the center-of-mass energy $\sqrt{s}$, which as previously discussed is the energy available for the production of new particles. In each case it is given by [22, 34]:

$$\begin{aligned}
\text{Center of mass:} \quad & \sqrt{s} = E_1 + E_2 = 2E_{beam}, \\
\text{Fixed target:} \quad & \sqrt{s} = [m_1^2 + m_2^2 + 2(E_1 m_2)]^{1/2} \sim \sqrt{2 m_2 E_{beam}}.
\end{aligned} \tag{2.13}$$

This means that colliding beam machines reach a high center-of-mass energy more easily than in a fixed target experiment, precisely because in these machines the laboratory reference frame is the same as the CM reference frame. In a fixed-target experiment, momentum conservation

[3] We are considering the Einstein dispersion relation: $E^2 = m^2 + \mathbf{p}^2$.

implies that the final state particles are always produced with a large kinetic energy, resulting in a significant portion of the initial energy being effectively wasted.

Particle accelerators use electric and magnetic fields to accelerate particles and control their trajectories, therefore only charged stable particles can be accelerated to high energies. This means that in general colliding machines are electron–positron colliders (e^+e^-), hadron colliders (pp or $p\bar{p}$) and electron–proton colliders (e^-p or e^+p), as can be seen in Table 3. Furthermore, one of the crucial factors for the energy of collision is the energy lost during the acceleration through the synchrotron radiation, which is a electromagnetic radiation that is emitted when charged particles travel at relativistic speeds through a magnetic field and are forced to change direction. For a particle of mass m, and energy E = γm, traveling in a circular orbit of radius R, the energy loss per revolution is [21, 34]:

$$\Delta E \propto \frac{1}{R}\left(\frac{E}{m}\right)^4. \tag{2.14}$$

Therefore a circular accelerator is more energy efficient for larger radius, more massive particles and a lower beam energy. The mass of a hadron is much greater than the mass of an electron ($m_p/m_e \sim 10^3$). Therefore for the same beam energy and circular orbit, a hadron collider reaches higher center-of-mass energies $\sqrt{s}$ in comparison with a lepton collider, precisely because a hadron collider does not lose much energy due to synchrotron radiation.

Moreover, other factors impact the center-of-mass energy in a collision. Since a hadron is composed of partons (gluons, quarks, antiquarks), in a hadron collider the processes of interest are those involving hard scattering collisions between the partons directly, this means that only a fraction of the momentum of each hadron is used in this collision [36]:

$$p_1^\mu = x_1 P_1^\mu \quad ; \quad p_2^\mu = x_2 P_2^\mu. \tag{2.15}$$

According to the parton model, x_1 and x_2 are distributed probabilistically and independently[4]. However, in the case of lepton colliders the full center-of-mass energy is available, as the leptons involved in the collision are not composite particles like the hadrons.

For these reasons, if the experiment aims to reach higher center-of-mass energies, the collider design should be chosen to minimize energy losses associated with the types of particles being collided. In this case, lepton colliders may benefit more from being linear and long, while hadron colliders may benefit from being circular with large R. It is important to emphasize that this is not always the case, colliders such as LEP and KEKB for example are lepton colliders but are not linear, the choice of parameters for a collider depends greatly on the objective of the experiment, the energy it will operate and several other factors.

[4] The probability that the momentum fraction of the first hadron is x_1 is independent of the second hadron.

Collider	$\sqrt{s}$ (GeV)	$\mathcal{L}$ ($cm^{-2}s^{-1}$)	Year	Laboratory
Tevatron ($p\bar{p}$)	1960	4.3×10^{32}	1987-2012	Fermilab
SLC (e^-e^+)	91.2	2.5×10^{30}	1989-1998	SLAC
LEP (e^-e^+)	$91.2 - 209$	10^{32}	1989–2000	CERN
HERA ($e^{\pm}p$)	320	7.5×10^{31}	1992-2007	DESY
KEKB (e^-e^+)	10.6	2.1×10^{34}	1999-2010	KEK
LHC (pp)	14000	2.1×10^{34}	2009-	CERN

Table 3 – Some recent hadron and lepton colliders and their characteristics [21, 22].

In a collider, particle collisions do not happen continuously over time, the focused beams are formed by particles distributed in bunches with approximately Gaussian distributions, and it is these discrete bunches of particles that collide with each other and generate the particles in the final state that are measured in the detector. Some important parameters in this configuration are the time-spacing between bunches t, the bunch crossing frequency $f = 1/t$, the effective cross-sectional area of the beams A at the interaction point, and the number of particles in each collided bunch N_a and N_b, where a and b label each of the beams. One of the important parameters in a collider is the instantaneous luminosity, which measures the rate at which particles are colliding per unit area per unit time, and is giving by [21, 34]:

$$\mathcal{L} = f\frac{N_a N_b}{A}. \tag{2.16}$$

Conventionally the instantaneous luminosity is given in units of $cm^{-2}s^{-1}$. If we are interested in calculating the reaction rate, witch is the rate at which a given event is produced at a collider, assuming that σ_{int} is the total scattering crossection of the process of interest, we can use the instantaneous luminosity and find that the reaction rate is given by:

$$R_{int} = \sigma_{int}\mathcal{L}. \tag{2.17}$$

This way we can also calculate the events of interest N_{int} generated, integrating $\mathcal{L}$ over the data-taking time of the collider, we find that:

$$N_{int} = \sigma_{int}\int \mathcal{L}(t)dt = \sigma_{int}L. \tag{2.18}$$

The L factor is known as integrated luminosity, and is typically measured in units of inverse barns (b^{-1}). The equation (2.18) implies that if we know σ_{int} it is possible to estimate how long a collider needs to run to collect the desired number of events. The integrated luminosity is a critical factor in the design and goals of an experiment, a higher integrated luminosity increases the likelihood of observing rare processes, furthermore different experiments or different runs of the same experiment can be compared using integrated luminosity to understand which collected more data or had better performance.

It is important to note that even if we have the total number of detected events of interest, this number still does not represent the actual value produced in the collisions. This is because the equipment is not perfect, for example the detector only covers a fraction of the total solid angle, so particles that fall outside this range are not detected. Additionally, there is a probability that particles passing through the detector may not be detected or correctly identified by the software. To account for these experimental issues, the concept of detector efficiency ϵ is defined, witch is the number of detected events divided by the actual number of events that occurred within the detector.

2.4 Detector and Kinematic variables

In a colliding beam experiment charged particles are accelerated until they have the energy to collide, this collision is designate to occur within a detector, which reconstructs the energies and momentum of these particles in order to understand what happened in the collision. A particle detector consists of multiple layers of material to detect different types of generated particles, as can be seen in Figure 4. The inner layer contains the tracking detector, made of many silicon pixels and strips, it is used to reconstruct the paths of charged particles that ionize the material. Additionally, a magnetic field is applied to curve the trajectory of the charged particles, providing information about their momentum [36, 37].

The other layers are made up of calorimeters, which are primarily used for particles to deposit part or all of their energy so that the particle's energy can be measured. Some examples found in detectors are the electromagnetic calorimeter (ECAL), used to detect photons and e^+/e^-, and the hadronic calorimeter (HCAL), used to detect hadrons which interact via the strong force. Additionally, there are particles that penetrate beyond the HCAL, such as muons and weakly interacting particles like the neutrinos. Since muons are about 200 times heavier the electrons their trajectory is much longer, allowing them to be tracked further in a dedicated muon chamber detector. However, not all particles are detected, such as neutrinos and particles that pass through the beampipe or gaps in the detector. These particles contribute to the missing-energy and missing three-momentum components.

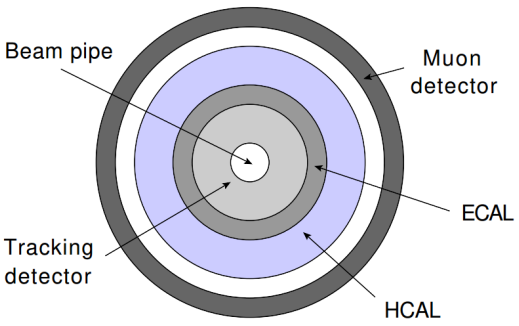

Figure 4 – Cross-sectional view of the internal layers of a detector in a colliding beam experiment [37].

In general the particle beam line is labeled as the z axis, so that the axes x, y form the transverse plane, in addition we will consider a cylindrical detector around the beam line as shown in Figure 5. In this system, the three-momentum of a particle is $\mathbf{p} \equiv (p_x, p_y, p_z)$, and it can be decomposed into a longitudinal component p_z along the z axis, and a transversal component $\mathbf{p}_T \equiv (p_x, p_y)$ in the transversal plane, where $|\mathbf{p}_T| = \sqrt{p_x^2 + p_y^2}$.

To understand the angular separation between the generated particles we can use the **azimuthal angle** ϕ around the cylinder varying between $[0, 2\pi)$, and the **polar angle** θ is the angle between the particle direction and the beam axis, and it varies between $[0, \pi]$. These variables are given by:

$$\phi = tan^{-1}\left(\frac{p_y}{p_x}\right), \tag{2.19}$$

and

$$\theta = tan^{-1}\left(\frac{|\mathbf{p}_T|}{p_z}\right). \tag{2.20}$$

In a hadronic collider the longitudinal momentum of the initial state partons are unknown, in other words the sum of the momentum p_z of those particles is not necessarily zero. This means that variables like θ do not have the same value in the laboratory reference frame and in the CM reference frame. In lepton colliders both the center-of-mass energy $\sqrt{s}$ and longitudinal momentum of the initial state are fixed, so that the total longitudinal momentum is most often zero. To address this issue when using the variable p_z, particularly in hadron colliders, it is essential to define variables that remain invariant under Lorentz boosts along the z-axis [38].

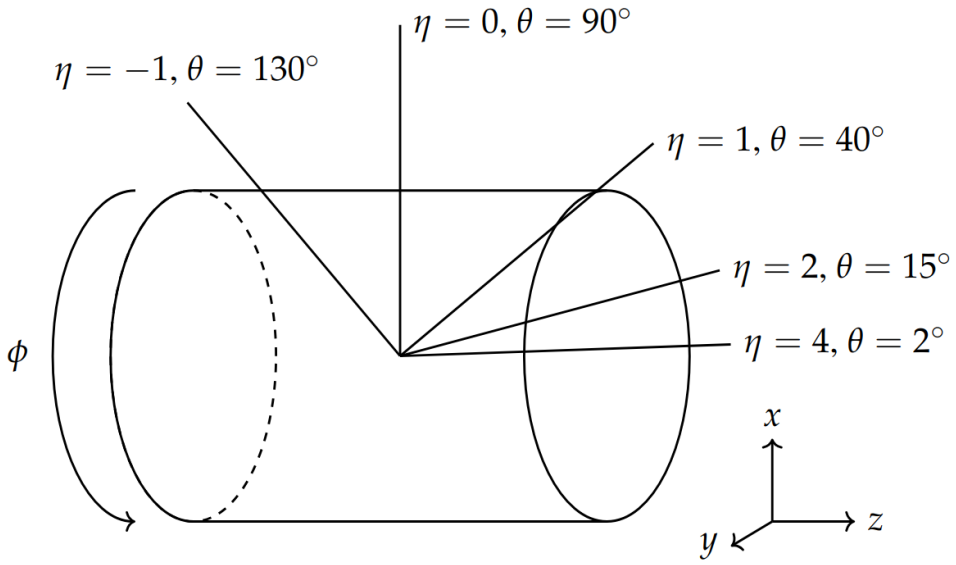

Figure 5 – Diagram of a cylindrical detector with indication of the Cartesian coordinates, in addition to the variables: pseudorapidity η, polar angle θ, and azimuthal angle ϕ. Inspired by [36].

To see how this occurs, let us consider how a four-momentum $p = (E, p_x, p_y, p_z)$ transforms under a Lorentz boost in the z direction [36, 37]:

$$p^\mu \rightarrow p'^\mu = \Lambda^\mu_\nu p^\nu, \tag{2.21}$$

knowing that

$$(\Lambda^\mu_\nu) = \begin{pmatrix} \gamma & 0 & 0 & -\beta\gamma \\ 0 & 1 & 0 & 0 \\ 0 & 0 & 1 & 0 \\ -\beta\gamma & 0 & 0 & \gamma \end{pmatrix}, \tag{2.22}$$

where $\beta = v$ and $\gamma = (1 - v^2)^{-1/2}$ in natural units, and v is the speed associated with the boost. The four-momentum p' is therefore given by:

$$\begin{pmatrix} E' \\ p'_x \\ p'_y \\ p'_z \end{pmatrix} = \begin{pmatrix} \gamma(E - \beta p_z) \\ p_x \\ p_y \\ \gamma(p_z - \beta E) \end{pmatrix}. \tag{2.23}$$

Hence the transverse moment $\mathbf{p}_T = (p_x, p_y) = (p'_x, p'_y)$ is boost invariant, however p_z and E are not. It is convenient to replace them with new variables, one of the most used is **rapidity**, which is defined as:

$$y \equiv \frac{1}{2} ln \left(\frac{E + p_z}{E - p_z} \right). \tag{2.24}$$

Applying the boost to z given by the equation (2.23) we find that:

$$\begin{aligned} y \rightarrow y' = \frac{1}{2} ln \left(\frac{E' + p'_z}{E' - p'_z} \right) &= \frac{1}{2} ln \left(\frac{(1-\beta)(E + p_z)}{(1+\beta)(E - p_z)} \right) \\ &= y + \underbrace{\frac{1}{2} ln \left(\frac{1-\beta}{1+\beta} \right)}_{Boost\ invariant}. \end{aligned} \tag{2.25}$$

This means that differences in rapidity have the same value in any reference frame that undergoes Lorentz boosts in the z direction:

$$\Delta y = y' - y = \frac{1}{2} ln \left(\frac{1-\beta}{1+\beta} \right). \tag{2.26}$$

The meaning of rapidity is related to how forward or backward the produced particle is with respect to the z direction. If the rapidity is zero $y = 0$ the particle is produced centrally, if it

is positive $y > 0$ the particle is closer to the $+z$ direction, being exactly in the $+z$ direction when $y \to \infty$, the rapidity behaves similarly for $y < 0$. If we are dealing with ultra-relativistic particles, as is the case in colliders, we can consider particles in the limit $E \gg m$ so that $E \approx |\mathbf{p}|$, therefore if $p_z = |\mathbf{p}| cos\theta$, then:

$$p_z \approx E cos\theta, \tag{2.27}$$

applying this result in to the rapidity (2.24), and considering the relationship $tan^2\left(\frac{\theta}{2}\right) = \frac{1-cos\theta}{1+cos\theta}$, we find that:

$$y \approx \frac{1}{2} ln\left(\frac{E(1+cos\theta)}{E(1-cos\theta)}\right) = \frac{1}{2} ln\left(\frac{1+cos\theta}{1-cos\theta}\right) = -ln\left(tan\frac{\theta}{2}\right). \tag{2.28}$$

Therefore we can define that when $E \gg m$ then $y \approx \eta$, so that η is known as **pseudorapidity**:

$$\eta = -ln\left(tan\frac{\theta}{2}\right). \tag{2.29}$$

This is a useful variable because it is a function only of the polar angle θ, which can be precisely measured experimentally. Pseudorapidity is equal to rapidity only for massless particles, and for massive particles, differences in pseudorapidity are not invariant under boosts. Different values for the pseudorapidity η and the polar angle θ in a detector can be found in Figure 4 as a reference.

Another useful variable in colliders is the **invariant mass**, it can be used to reconstruct the mass of a intermediate particle that cannot be observed directly by the detector, as for example in the resonant process in which a Z is generated and decays into leptons. The invariant mass of two particles with four-momentum p_1 and p_2 is [36, 38]:

$$m = \sqrt{(E_1 + E_2)^2 - (\mathbf{p}_1 + \mathbf{p}_2)^2}. \tag{2.30}$$

However, we often cannot reconstruct the entire three-momentum of the particles because of the p_z component, therefore it is possible to define the invariant mass as beeing a function of only the transverse momentum $\mathbf{p}_T$. This variable is known as **transverse mass**, and is given by:

$$m_T \equiv \sqrt{(E_T^1 + E_T^2)^2 - (\mathbf{p}_T^1 + \mathbf{p}_T^2)^2}, \tag{2.31}$$

where E_T is the **transverse energy** of the particles, which is also a function of the transverse momentum $\mathbf{p}_T$:

$$E_T \equiv \sqrt{m^2 + |\mathbf{p}_T|^2}. \tag{2.32}$$

If particles are generated purely in the transverse direction $(\eta = 0)$, then $m_T = m$. However, if they have any other component in the z direction, the transverse mass will always be $0 < m_T < m$.

We are often only interested in the direction in which the final state particle was produced. Each direction is associated with a single point in the cylindrical detector, and we can fully specify this point using the pseudorapidity η and the azimuthal angle ϕ around the detector. This way, we can define the **angular separation** between two particles as being:

$$R = \sqrt{(\Delta\phi)^2 + (\Delta\eta)^2}. \tag{2.33}$$

This angular separation is boost invariant. Therefore, to describe events mainly in a hadronic collider it is important to use kinematical variables such as (p_T, η, ϕ), for relativistic speeds we have that $E_T \approx p_T = Echos\theta = Ecosh^{-1}\eta$. These events are usually described in a **lego plot**, so that the plane is formed by ϕ, η and the height by the transverse energy E_T. An example of a lego plot of an event in ATLAS can be seen below:

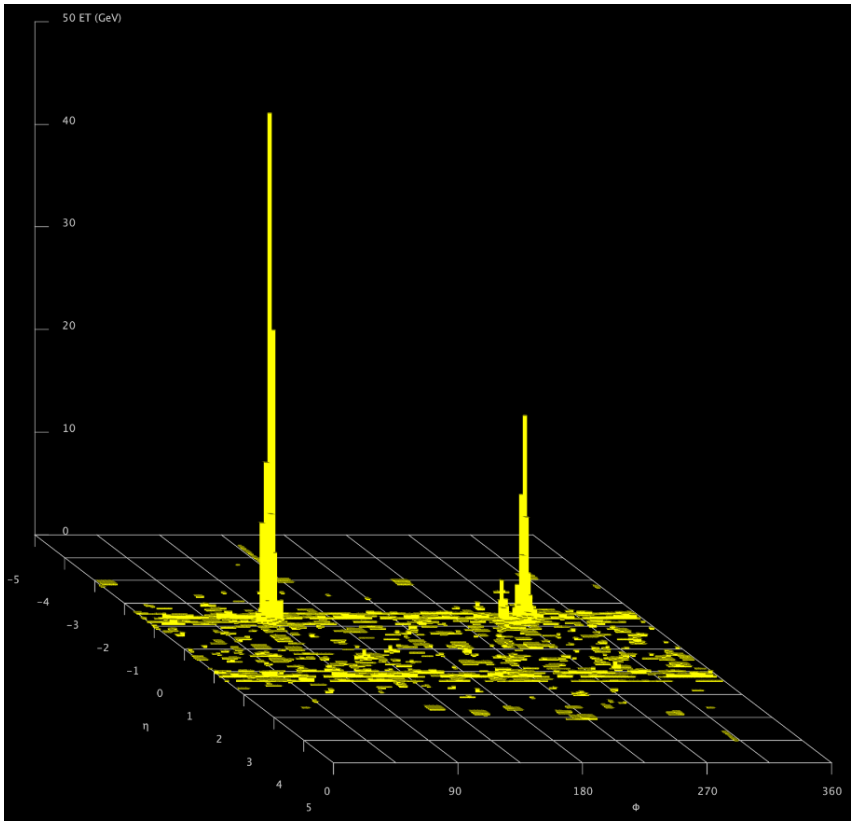

Figure 6 – Display of a di-jet event (Run number 475522, Event number 2563184864) recorded by ATLAS on Monday, the 13th of May 2024. The jets are high-energy, collimated (tall, narrow spikes) and are shown in a lego plot, which displays energy deposits in the calorimeter of the unrolled cylindrical detector [39].

2.5 Z boson

Now that we have discussed the main characteristics of colliders, their most relevant kinematic variables and how a detector works, we will focus our discussion on the processes of interest in discovering the properties of the Z boson. This discussion is especially important for this work because our simulations made for the future CLIC collider are related to e^+e^- collisions, and have as signal processes mediated by a Z' boson with very similar characteristics to the Z boson in the SM.

The electroweak theory made significant predictions about the properties of vector bosons, but it was necessary to test these predictions experimentally. To do so, the Large ElectronPositron Collider (LEP) was used, an experiment built at CERN consisting of a 27 km circumference ring, and it is the most powerful lepton accelerator ever built. As the name suggests, it collides electrons with positrons at energies that could reach up to 209 GeV as seen in Table 3. By reaching this energy, LEP conducted precise measurements to test the electroweak theory, including the masses of the Z and W bosons, solidifying the validity of the SM [22, 40].

2.5.1 Resonance

As previously discussed in Chapter 1, the Z boson is a neutral particle that couples to all flavors of fermions, making it reasonable to assume that any fermion annihilation process mediated by a photon in QED is also applicable to the Z boson. The theoretical predictions for the Z boson were experimentally verified with high precision using the LEP Collider, particularly through electron annihilation processes such as $e^+e^- \to \mu^+\mu^-$. The lowest-order Feynman diagrams for this annihilation process are shown below:

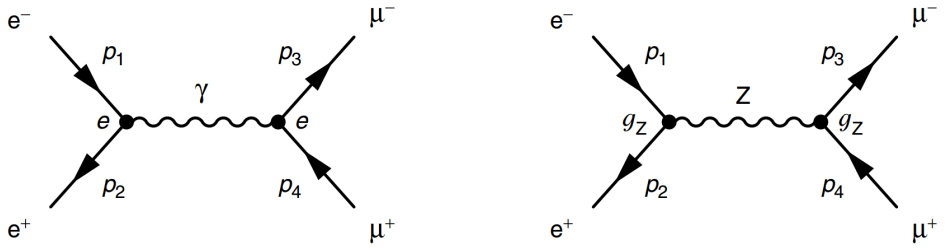

Figure 7 – Lowest order Feynman diagrams for the annihilation process $e^+e^- \to \mu^+\mu^-$ [22].

To calculate the total cross-section for the annihilation process it is necessary to take into account two amplitudes, which arise from the exchange of photons γ and Z bosons in the s-channel, which are proportional to:

$$\mathcal{M}_\gamma \propto \frac{e^2}{q^2} \quad ; \quad \mathcal{M}_Z \propto \frac{g_Z^2}{q^2 - m_Z^2}. \tag{2.34}$$

Based on the center-of-mass energy, we can conclude that for $\sqrt{s} \gg m_Z$ both processes are equally significant, if $\sqrt{s}\ m_Z$ the process involving the Z boson is predominant, and for

$\sqrt{s} \ll m_Z$ the photon-mediated process is dominant. Thus, it is possible to arrive at an expression for the cross-section of the process $e^+e^- \to Z \to \mu^+\mu^-$, with $q^2 = s$, so that it is proportional to:

$$\sigma \propto |\mathcal{M}|^2 \propto \left| \frac{1}{s - m_Z^2 + i m_Z \Gamma_Z} \right|^2 = \frac{1}{(s - m_Z^2)^2 + m_Z^2 \Gamma_Z^2}, \tag{2.35}$$

where Γ_Z is the decay width of the Z boson and the amplitude is $|\mathcal{M}|^2 = |\mathcal{M}_\gamma + \mathcal{M}_Z|^2$. The behavior of the cross-section as a function of the center-of-mass energy for processes involving quarks in the final state $e^+e^- \to q\bar{q}$ is shown in the figure below.

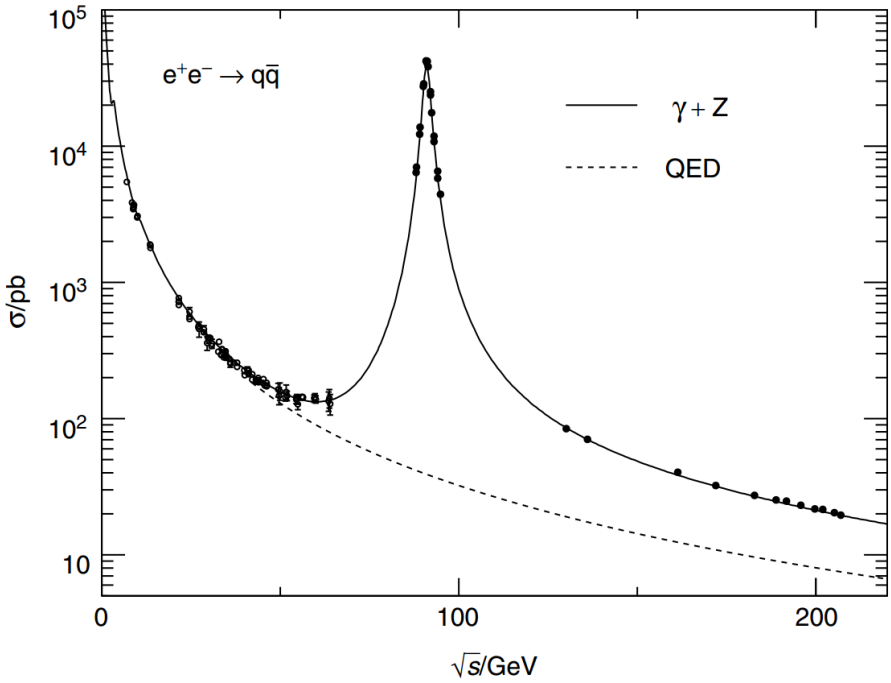

Figure 8 – Contribution of QED process and Z boson for the process $e^+e^- \to q\bar{q}$ in terms of cross-section at LEP close to and above Z resonance, and lower-energy measurements from earlier experiments [22].

This means that for center-of-mass energies between 50 and 80 GeV, both processes play a significant role. However, as the energy approaches the resonance at approximately 90 GeV the Z boson process dominates, exceeding the QED contribution by about three orders of magnitude. For $\sqrt{s}$ beyond the resonance the contributions from QED and the Z boson become comparable, reflecting the unification of the electroweak theory where $g_Z \sim e$.

2.5.2 The Z mass

For the precise measurement of the Z boson mass at the LEP collider, it was necessary to incorporate two additional higher-order QED diagrams in addition to the first-order diagrams shown in the Figure 7. These diagrams consider a phenomenon known as Initial State Radiation

(ISR), where a photon is emitted from the initial state particles. The tree-level diagram, along with the higher-order diagrams are shown below.

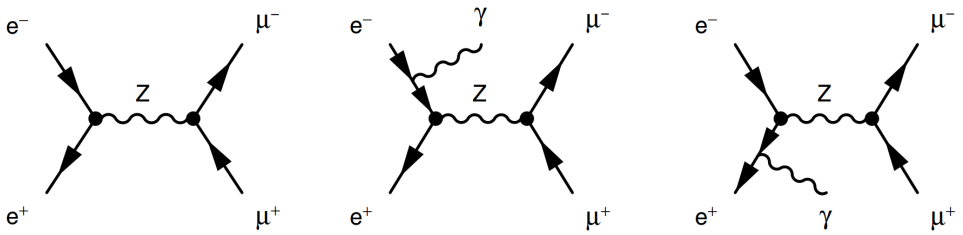

Figure 9 – Feynman diagrams for the process $e^+e^- \to \mu^+\mu^-$ with initial state radiation, and the tree-level diagram [22].

The emission of this photon modifies the center-of-mass energy $\sqrt{s}$, and therefore also affects the Z resonance curve. The effective s mandelstam variable must be redefined as s' considering the energy loss due to this radiation, which is given by the square of the sum of four-momenta of the e^+ and e^- after the ISR, so that:

$$s' = (p_1 + p_2)^2 = (2E - E_\gamma)^2 - E_\gamma = 4E^2\left(1 - \frac{E_\gamma}{E}\right) = s\left(1 - \frac{E_\gamma}{E}\right), \tag{2.36}$$

where E is the initial total energy, and E_γ is the energy of the emitted photon. Therefore, the distribution of the center-of-mass energy can be expressed in terms of the normalised probability distribution given by $f(s', s)$. Substituting this function into:

$$\sigma_{means}(s) = \int \sigma(s')f(s', s)ds', \tag{2.37}$$

where

$$\sigma\left(e^+e^- \to Z \to \mu^+\mu^-\right) = \frac{12\pi s}{m_Z^2}\frac{\Gamma_{ee}\Gamma_{\mu\mu}}{(s - m_Z^2)^2 + m_Z^2\Gamma_Z^2}. \tag{2.38}$$

It is obtained by analyzing the cross-section as a function of $\sqrt{s}$ values shown in Figure 10. The impact of Initial State Radiation (ISR) is to distort the observed Z resonance. However, since ISR is a QED process, the function $f(s', s)$ can be computed with high precision. Near and below the resonance peak, ISR reduces the measured cross section as the center-of-mass energy shifts further from the peak at the e^+e^- vertex. On the other hand, above the resonance peak the ISR increases the cross section by bringing the average center-of-mass energy closer to the peak. With these considered, the following mass value for the Z boson was achieved:

$$m_Z = 91.1875 \pm 0.0021 \text{ GeV}. \tag{2.39}$$

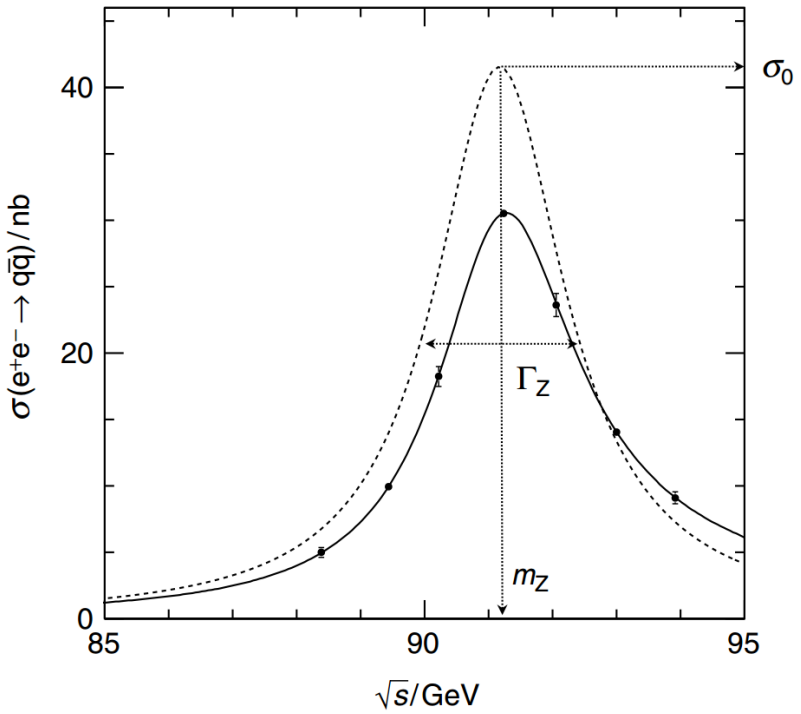

Figure 10 – Cross section for the process $e^+e^- \rightarrow q\bar{q}$ from LEP with the correction of ISR in the dashed curve [22].

2.5.3 The Z width

Taking into account the effects of ISR as shown in Figure 10, it is found that the total decay width of the Z boson is:

$$\Gamma_Z = 2.4952 \pm 0.0023 \text{ GeV} \tag{2.40}$$

Recalling that the total width is the sum of the partial widths, such that:

$$\Gamma_Z = \Gamma_{ee} + \Gamma_{\mu\mu} + \Gamma_{\tau\tau} + \Gamma_{\text{hadrons}} + \Gamma_{\nu_e\nu_e} + \Gamma_{\nu_\mu\nu_\mu} + \Gamma_{\nu_\tau\nu_\tau}, \tag{2.41}$$

Rewriting this expression, results in:

$$\Gamma_Z = 3\Gamma_{ll} + \Gamma_{\text{hadrons}} + 3\Gamma_{\nu\nu}. \tag{2.42}$$

Assuming that we are uncertain about the existence of additional generations of neutrinos, we can then write that:

$$\Gamma_Z = 3\Gamma_{ll} + \Gamma_{\text{hadrons}} + N_\nu\Gamma_{\nu\nu}. \tag{2.43}$$

Thus, it is possible to obtain an expression for the number of neutrino generations as follows:

$$N_\nu = \frac{(\Gamma_Z - 3\Gamma_{ll} - \Gamma_{\text{hadrons}})}{\Gamma_{\nu\nu}^{SM}} \tag{2.44}$$

and it is ultimately found that the number of light neutrino generations is given by:

$$N_\nu = 2.9840 \pm 0.0082 \tag{2.45}$$

The determination of the effective number of neutrinos from experimental results at LEP collider was of great importance because it aligns with the theoretical predictions of the Standard Model, which considers 3 neutrino generations. Additionally, this is relevant for a deeper understanding of elementary interactions and reinforces the ΛCDM cosmological model. Cosmological data provides constraints on neutrino properties, such as their mass, assuming that only massless or light (sub-keV) relic particles existed during the Big Bang Nucleosynthesis (BBN) epoch. After reviewing the key ingredients of collider physics, we will move to the main chapter of this dissertation.

3 Electron–positron colisions at CLIC considering a new Z' boson

In the preceding chapters, we introduced the Standard Model of particle physics and its structure, emphasizing key elements such as its particle content, the role of gauge invariance, and the necessity of spontaneous symmetry breaking to generate the mass of the particles. We also detailed the general characteristics of colliders, and explored its key parameters and useful kinematic variables used in these types of experiments, moreover we explored the properties of the Z boson, including its mass and decay width. All of this was aimed at establishing a solid theoretical foundation for our next discussions; in this chapter will delve into the discovery potential of a new Z' boson emerging of a simplified model known in the literature as the "leptophilic Z'". As previously discussed in the introduction, this work aims to be a study based on the paper "Searching for a Leptophilic Z' and a 3-3-1 Symmetry at CLIC"[1], which was chosen for its general approach in utilizing various concepts of collider physics, serving as a solid foundation for my introduction to the topic.

With this in mind, our investigation will unfold within the framework of the Compact Linear Collider (CLIC), a particle collider designed for e^+e^- collisions that will operate at a maximum center-of-mass energy of 3 TeV. The CLIC collaboration is projected to be a global cooperative effort situated within the CERN facilities [41], and its primary aim is to construct a linear e^+e^- collider operating at the TeV scale while maintaining high luminosity. In order to fully leverage its potential for BSM physics, CLIC is strategically designed to be implemented in progressive stages. The projected operational energies for each of CLIC's three stages are 380 GeV, 1.5 TeV, and 3 TeV, respectively. The anticipated spatial range for its footprint spans between 11 km and 50 km.

Recent times have witnessed significant advancements in the technical refinement and rigorous testing of CLIC accelerator systems. These breakthroughs have not only led to cost reductions in construction but have also enhanced the collider's physics capabilities. Set to commence operations around 2035, the inaugural beam injection heralds the beginning of an expansive physics program projected to unfold over 25 to 30 years. Drawing from the experience gained from the LEP collider [42, 43], CLIC emerges as a promising avenue for exploring physics BSM. With its high luminosity and increased center-of-mass energy, CLIC stands ready to facilitate direct investigations and enable precise measurements spanning a wide range of both SM and BSM processes. This potential is particularly relevant in the examination of the Higgs boson, expanded scalar sectors, new gauge bosons, and other phenomena.

Numerous theories beyond the Standard Model propose the existence of a neutral gauge

bosons that couple to leptons, and these theories provide potential explanations for unresolved phenomena such as dark matter, neutrino masses, the anomalous magnetic moment of the muon, and more. These neutral bosons are often linked to a new abelian gauge symmetry, one that undergoes spontaneous breaking, thus giving rise to a Z' boson with a mass approximating the scale of new physics. Alternatively, a Z' boson can emerge from non-abelian gauge symmetries. These Z' bosons can potentially manifest themselves in hadron and lepton colliders, generating dilepton resonances, for example. From an experimental point of view, a Z' boson essentially represents a resonance, possessing a higher mass compared to the Z boson. However, from the perspective of theoreticians, a Z' field embodies a new force carrier, showing the way for the exploration of BSM physics.

Motivated by the importance of Z' bosons in theoretical constructions, our goal is to evaluate CLIC's potential for discovering a leptophilic Z'. This new gauge boson arises within straightforward gauged lepton number theories [44, 45, 46], as well as in more intricate configurations [47, 48]. In the context of linear colliders, past studies have investigated leptophilic Z' bosons [49, 50, 51], however none of these efforts have focused on a sequential leptophilic Z' boson. This boson, which couples to SM leptons similarly to the Z boson but lacks interactions with quarks, remains unexplored.

Sequential Z' bosons are often the subject of collider searches at the LHC [52, 53, 54, 55, 56, 57]. If couplings with quark are removed or dwindled, a sequential leptophilic Z' naturally emerges as a consequence [58, 59, 60, 51, 61], potentially serving as a reference model at CLIC. Notably, in scenarios devoid of quark interactions, CLIC becomes a particularly promising avenue for exploration, despite the LHC surpassing it in reach due to its quark couplings. Furthermore, beyond its initial role in discovery, CLIC has the potential to evolve into a precision instrument after identifying a Z' boson, whether at the LHC or the HL-LHC.

Without CLIC data at present our analysis is limited to evaluating CLIC's sensitivity reach. To do this, we are going to investigate the optimal kinematic cuts on variables such as transverse momentum p_T, pseudorapidity η and electron-positron invariant mass $M(e^+e^-)$. This exploration aims to maximize signal efficiency and achieve a 5σ signal significance for a given luminosity. Before we begin our analysis, we are going to quickly show the main features of CLIC.

3.1 The Compact Linear Collider

The Compact Linear Collider, a project currently being developed by the CLIC accelerator collaboration at CERN, is designed as a high-luminosity e^+e^- linear collider with the potential to achieve multi-TeV energies. A distinctive innovation within CLIC is the adoption of the two-beam acceleration technique, employing normal conducting accelerating structures operating in the range of $70 - 100$ MeV/m.

The Conceptual Design Report (CDR) for CLIC was made public in 2012 [62]. Its central aim was to establish the feasibility of the CLIC accelerator for reach energies up to 3 TeV. Just as LEP and SLAC were important to test various SM predictions [42, 43], CLIC envisions a span of 27 years [63], divided into three distinct yet complementary stages, dedicated to gathering more precise electroweak measurements and identifying signals of new physics.

Employing an innovative acceleration mechanism, CLIC aspires to gradually attain energies up to $\sqrt{s} = 3$ TeV along a staged progression, along with an integrated luminosity of 5 ab^{-1}. In its initial operational phase, CLIC is anticipated to work at an energy of $\sqrt{s} = 380$ GeV and a luminosity of 1 ab^{-1}. In the subsequent second and third stages, operation is projected at $\sqrt{s} = 1.5$ TeV with $L = 2.5$ ab^{-1}, and $\sqrt{s} = 3$ TeV with $L = 5$ ab^{-1}, respectively [64]. At each of these operational stages, the CLIC program strives to refine electroweak precision measurements of SM parameters and potentially identify both direct and indirect indications of new physics [65, 66].

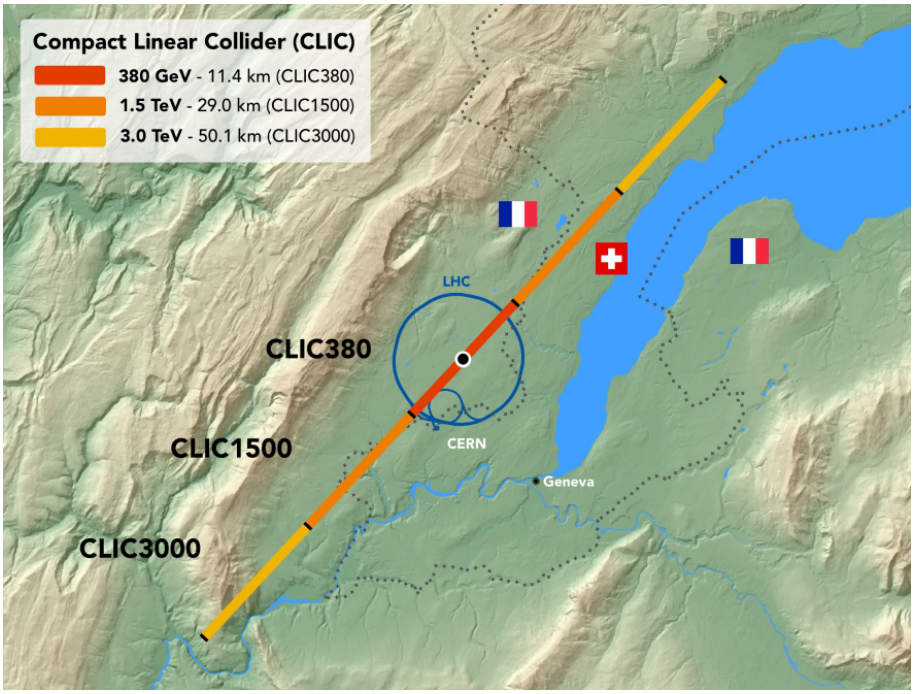

Figure 11 – Diagram of the CLIC near CERN, showing the three stages of implementation [41].

These stages in which the CLIC experiment will work are designed according to findings derived from the HL-LHC investigations. Specifically, adjustments to the center-of-mass energy can be achieved through elongating the accelerator's length or enhancing acceleration methodologies. This distinctive approach to acceleration technology within the CLIC experiment retains the potential for conducting inquiries characterized by elevated center-of-mass energy and luminosity. Having in mind the new physics potential of CLIC and the popular presence of Z' fields in theoretical constructions, the next section will briefly describe the model used in this work.

3.2 The Model

As previously mentioned, this chapter focuses on studying the capability to produce and detect a new Z' boson at CLIC experiment. The model employed for this analysis is the Z' leptophilic model, which presents itself as a potential and straightforward extension to the SM. A sequential leptophilic boson is a boson that only interacts with leptons, in addition the interactions with quarks are suppressed or negligible, and will not be considered in this work. Furthermore, because it is sequential this means that the boson has couplings to SM leptons equal to the Z boson, this unique attribute could lead to distinctive collider phenomenology—observable signals, that can be detected in high-energy particle collider experiments. The amplified couplings between the Z' boson and leptons may result in distinct decay patterns, production rates, and other measurable phenomena. These characteristics hold the potential for exploration in forthcoming lepton colliders, such as CLIC.

As the leptophilic Z' has the same couplings with the leptons as the SM's Z, we are going to use the part of the SM neutral current lagrangian corresponding to this interaction:

$$\mathcal{L} = -\frac{g}{2cos\theta_W}\sum_i \bar{\psi}_i\gamma^\mu(g_V^i - \gamma^5 g_A^i)\psi_i Z'_\mu \tag{3.1}$$

where $\theta_W = tan^{-1}(g'/g)$, $g_V^i = T^3 - 2Qsin^2\theta_W$, and $g_A^i = T^3$, as discussed in equation (1.123). In this case, $i = 1, 2, ..6$; with ψ_i running over all six lepton flavors. This new boson can potentially couple new particles but we hypothesize that these new particles are too heavy to be produced at CLIC via Z' exchange. The lagrangian above is, therefore, the relevant one for phenomenological studies. As a result of these leptophilic Z' coupling considerations, the total decay width $\Gamma_{Z'}$ is narrower, significantly influencing the number of events of the signal that we will describe in the next subsection.

3.3 Simulation and Analysis

The simulation of all signal and background events was carried out using FEYNRULES [67], MADGRAPH5 [68], PYTHIA8 [69], and DELPHES3 [70]. A total of 80000 events were generated for each Z' mass parameter, while 200000 events were generated for backgrounds. In order to simulate realistic e^+e^- collider environments at CLIC, we utilized the clic3000ll PDF set. We do not consider the interference between the SM and the Z' since the ratio $\Gamma_{Z'}/m'_Z$ is small, amounting to only a few percent.

The SM background and the signal involve s and t-channel diagrams that exchange a Z boson or A (photon) for the background and a Z' boson for the signal. These diagrams are illustrated in Figure 12. In order to mitigate collinear divergences, we generated events that fulfill the subsequent fundamental selection criteria:

$$p_T > 100 \text{ GeV} \quad ; \quad |\eta| < 3, \tag{3.2}$$

for both electron and positron in the event.

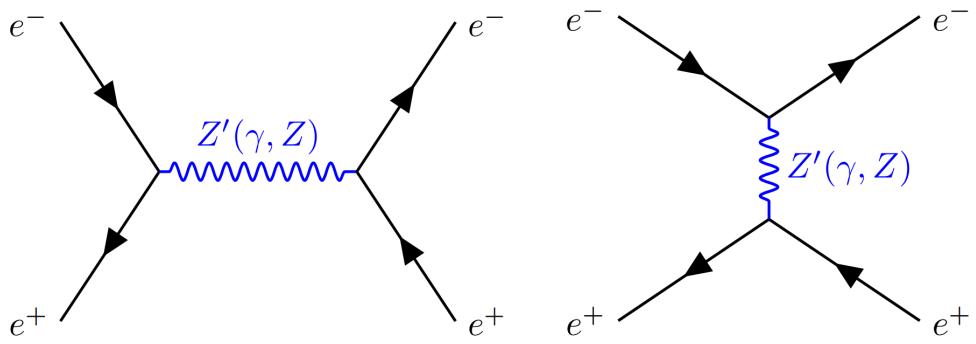

Figure 12 – Feynman diagrams for the signal (Z') and background (A, Z) processes in the s-channel and t-channel [1].

The production cross section times branching ratio into e^+e^-, after applying the basic cuts of Equation (3.2), for the leptophilic Z' boson is presented in Figure 13, plotted as a function of the Z' mass. For masses much smaller than the collider energy, the t-channel diagram dominates as the Z' is produced off its mass shell. However, heavier Z' bosons tend to be produced closer to the mass shell, leading to an increased cross section towards $M_{Z'} = 3$ TeV, and subsequent decrease for larger masses.

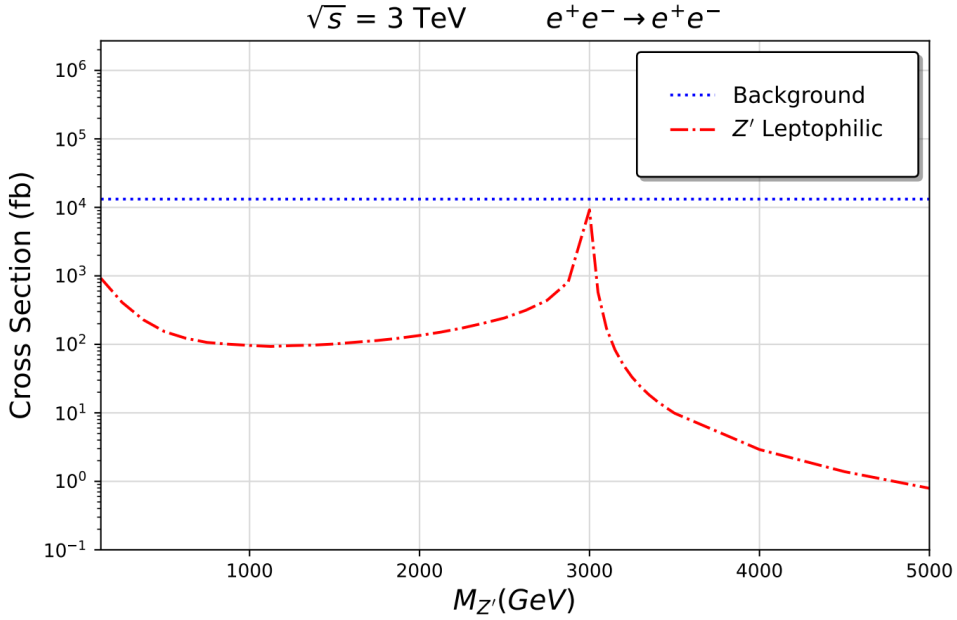

Figure 13 – The $e^+e^- \to e^+e^-$ cross section (red dashed lines) for Z' masses up to 5 TeV. The SM background is displayed as a dotted blue curve.

The branching ratio of the process $BR(Z' \to e^+e^-)$ is 11%, within the mass range considered in this study. The SM crossection for $e^+e^- \to e^+e^-$ is 13.2 pb after applying the cuts of of Equation (3.2). The signal and background distributions for the transverse momentum

p_T, rapidity η and the invariant mass $M(e^+e^-)$, used for cuts, are displayed in Figure 14. As we observe, the characteristics of signal and background are notably distinctive, particularly for heavy Z' bosons. However, in the case of lighter Z', the peaks in the e^+e^- invariant mass reveal the presence of signals, differentiating them from the smooth background spectrum.

Regarding the rapidity distributions, lighter Z' particles and the SM backgrounds exhibit a comparable behavior, with the majority of events being concentrated in the high rapidity regions of the detector. On the contrary, heavy Z' bosons produce central electrons and positrons. This phenomenon arises due to the interplay between the s and t-channel amplitudes. The t-channel contribution is accentuated when the final-state lepton is collinear with the initial-state one, while the s-channel yields high-p_T outcomes.

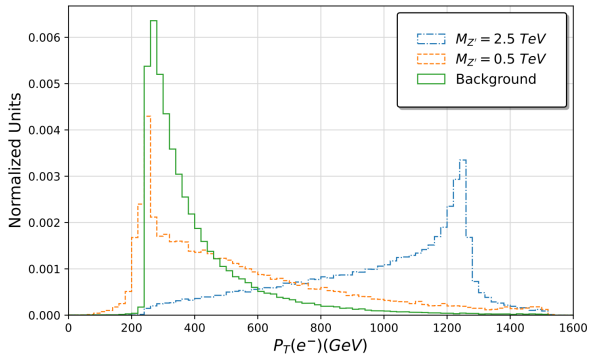

(a) Signal and background distributions for the transverse momentum of electrons in the final state corresponding to Z' masses of 0.5 and 2.5 TeV.

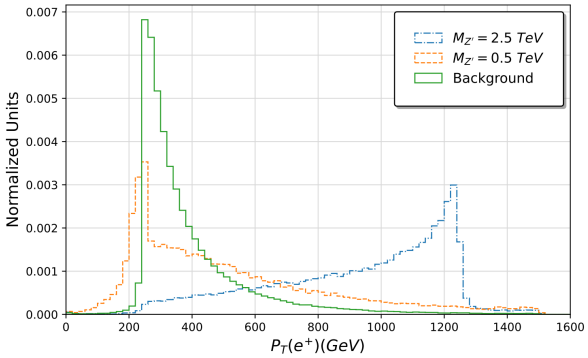

(b) Signal and background distributions for the transverse momentum of positrons in the final state corresponding to Z' masses of 0.5 and 2.5 TeV .

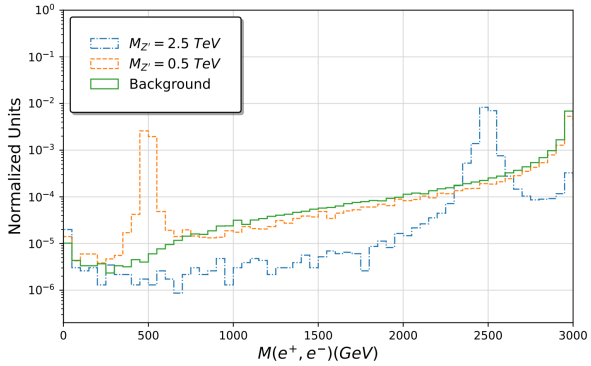

(c) Signal and background distributions for the invariant mass of an electron-positron pair in the final state corresponding to Z' masses of 0.5 and 2.5 TeV.

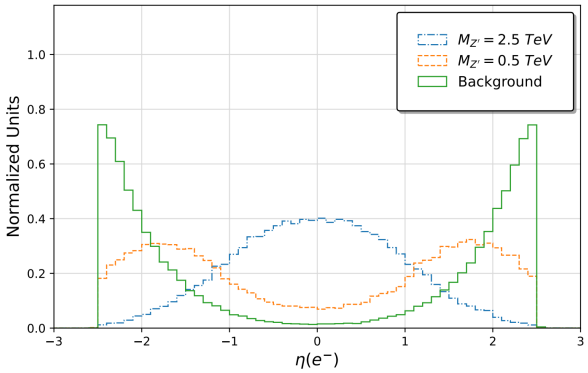

(d) Signal and background distributions for the pseudorapidity of electrons in the final state corresponding to Z' masses of 0.5 and 2.5 TeV.

Figure 14 – Signal and background distributions for different kinematic variables corresponding to a Z' leptophilic boson with masses of 0.5 and 2.5 TeV.

In order to mitigate backgrounds and enhance the statistical significance of the signal, we sought optimal kinematic cuts on p_T, η and $M(e^+e^-)$ that simultaneously maximize signal efficiency and minimize background contamination. As detailed in the subsequent section, the optimization process yielded negligible background efficiencies for Z' masses spanning from 10

GeV to 3 TeV. Subsequently, we compute the signal significance using the following formula:

$$N_\sigma = \frac{L \times \epsilon_S \sigma_S}{\sqrt{L \times \epsilon_B \sigma_B + (\epsilon_B^{sys} \times L \times \epsilon_B \sigma_B)^2}} \tag{3.3}$$

Here, σ_S (ϵ_S) and σ_B (ϵ_B) represent the cross section (selection efficiency) of the signal and backgrounds, respectively. The integrated luminosity is denoted as L, while ϵ_B^{sys} stands for the systematic uncertainty in the background rate. In situations where no Monte Carlo background events fulfill the selection criteria, we conservatively assume a background rate indicated by σ_B / n_{MC}, where $n_{MC} = 2 \times 10^5$, the count of simulated background events.

3.4 Results and Discussions

Table 4 displays the optimal cuts for certain Z' masses. Here were analyzed the following kinematic variables: the electron and positron transverse momentum p_T, the electron and positron pseudorapidity η and the invariant mass of a electron-positron pair M_{ee}.

$M_{Z'}$	$p_T >$	$\lvert\eta\rvert <$	$\lvert M_{ee} - M_c\rvert < \delta_M$	ϵ_S (%)
500	236	2.20	441 ± 55	1.8
1000	445	2.13	1067 ± 54	9.3
1500	640	2.77	1541 ± 51	16.3
2000	519	1.28	1943 ± 79	14.5
2500	1038	1.91	2410 ± 85	10.1

Table 4 – The best kinematic cuts for different Z' masses.

In the table, M_c represents the central value on the invariant mass that increments the significance and δ_M is a number around the central value. So the algorithm gives as result the cut $\delta_M < M_c < \delta_M$ on the invariant mass. All the units are in GeV. The selection of the e^+e^- mass cut involved identifying the most suitable window around the signal peak to isolate events. For that, for every Z' mass, a total of 4×10^5 random searches were conducted within the parameter space of cut thresholds encompassing the kinematic variables p_T , $|\eta|$, and the e^+e^- proximate to the signal peak.

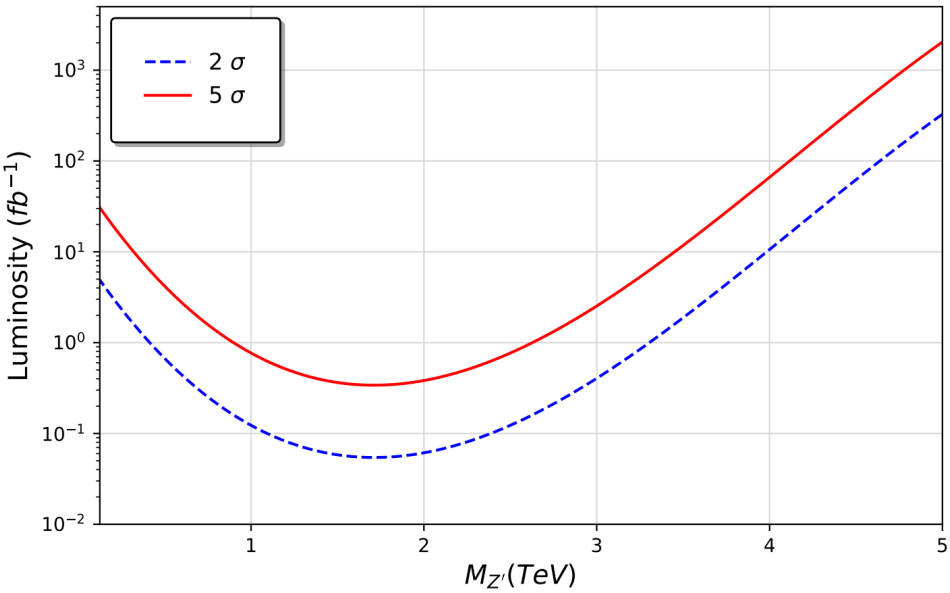

Figure 15 – Luminosity that the CLIC experiment needs to reach to detect a new Z' boson with 2σ (or 95% C.L.) in blue, and 5σ (or 99.99994% C.L.) in red.

Notably, the background efficiencies remain minimal across all Z' masses, while the signal efficiency demonstrates an ascending trend from lighter to heavier Z' bosons. We conclude that higher signal efficiencies are achieved by hardening the p_T threshold and selecting events that are more centrally produced in the detector.

The Figure 15 illustrates the luminosity required to potentially exclude a Z' at 95% confidence level (C.L.) or to discover it in the 3 TeV CLIC. Our findings show that CLIC can exclude Z' bosons up to 3TeV with less than $10fb^{-1}$ of integrated luminosity, and a 5 TeV Z' for an integrated luminosity of $300fb^{-1}$. We can also conclude that CLIC has the potential to discover a Z' with masses between 1-5 TeV with less than $1ab^{-1}$ of integrated luminosity.

Our findings could be improved with the inclusion of dimuon events which would in principle double the number of signal events and consequently enhance the significance. It is clear that CLIC can offer a complementarity probe to new physics to the LHC and other proposed future colliders.

4 Conclusions & Perspectives

In the first chapter, the Standard Model of electroweak interactions was introduced, providing a brief historical overview of how this model emerged and the main ideas and technologies that needed to be developed to shape it into its current form. The particle content of this model, including fermions, vector bosons, and the scalar Higgs boson, was presented, detailing their characteristics and respective Lagrangians. The concept of symmetries and gauge invariance was then introduced, along with Yang-Mills theories, which describe the self-interaction between the mediating bosons. The concept of spontaneous symmetry breaking was also discussed in the context of the Higgs mechanism, which serves as a fundamental process in the Standard Model, responsible for generating mass for the massive vector bosons, as well as for the fermions through the Yukawa sector. Finally, an analysis of the electroweak Lagrangian was conducted, examining the kinetic terms for particle propagation, their interaction terms, any possible self-interactions, and their mass terms, discussing and detailing the role of each term in the Lagrangian.

In the second chapter, we introduced collider physics from a theoretical approach, discussing the concept of cross section and providing an example of how to calculate this quantity in relation to a simple but relevant process for our work. Additionally, we discussed the Mandelstam variables, which are widely used in high-energy physics, mainly because they are Lorentz invariants and are related to the energies and momenta of the particles involved in a process. Afterward, we provided a general discussion on how particles are detected in a collider through detectors and the functions of their respective components. The main parameters of a collider were also discussed, including how different types of colliders and approaches influence the maximum center-of-mass energy achievable, with particular attention to the energy lost due to synchrotron radiation. Finally, we explored the concepts of instantaneous luminosity and integrated luminosity, as well as their importance as parameters for quantifying the data acquisition of a collider. We also covered the various kinematic variables used to process the signal data and provided a brief introduction to the physics of the Standard Model Z boson, with the aim of establishing a theoretical foundation for the discussions in the third chapter.

In the third chapter, we discussed the main characteristics of the future CLIC collider, such as the center-of-mass energies and integrated luminosity across its three phases of implementation, reaching a maximum of $\sqrt{s} = 3$ TeV and $L = 5$ ab^{-1}, as well as other technical specifications to provide a general idea of what is expected from the collider in the future. Afterward, a brief introduction to the model is provided, which features a Z' boson with the same couplings as the Standard Model Z boson but without interactions with quarks. This makes it a simple model that can naturally be implemented for e^+e^- collisions at CLIC. The model was implemented using FEYNRULES, and the collision data were generated through MADGRAPH5 and also with the help of CALCHEP. Final state radiation was considered by activating PYTHIA8,

and the conversion into detector events at CLIC was done using DELPHES3.

As a result of the simulation, the cross-section for the process $e^+e^- \to e^+e^-$ considering $\sqrt{s} = 3$ TeV shows a peak when $m_{Z'} = 3$ TeV, a result of the Z' resonance. For the pseudorapidity of the electrons, we observe that for $m_{Z'} = 2.5$ TeV, there is an excess of signal at $\eta = 0$, due to the high transverse momentum of the electrons at this mass. However, the opposite behavior occurs for a mass of $m_{Z'} = 0.5$ TeV, where the transverse momentum of the electrons is low, and thus they are distributed at high $|\eta|$, causing the signal events to mix with the background.

Using the signal significance equation (3.3) and applying a random search algorithm, we were able to find the best kinematic cuts for pseudorapidity η, transverse momentum p_T, and invariant mass $M(e^+e^-)$ that maximize the statistical significance of the signal for different Z' mass values. Finally, with this data, we were able to determine the expected integrated luminosity in the CLIC experiment necessary to observe a Z' signal with 95% C.L. or to achieve a Z' discovery with 5σ statistical significance.

In conclusion, this study provided valuable experience with several packages for collider event simulations, deepening our understanding of the steps needed to implement a BSM model in a simulator, process data to extract kinematic variables, and identify Z' boson signals. The work involved multiple analyses, significantly advancing our expertise in collider simulations. Moving forward, we plan to further enhance our programming skills, achieve proficiency in $C++$, and begin studying GEANT4, a crucial tool for simulating detectors, which will be essential for future projects at CERN. Initially, we aim to continue the CLIC research presented in this dissertation, expanding it to analyze a Z' model with dark matter. Subsequently, we will focus on research involving CERN detectors such as NA64 and ATLAS to explore dark sectors. In summary, given our plans to be associated with CERN, this dissertation was a great learning laboratory.

References

[1] ALVES, A. et al. Searching for a leptophilic Z' and a 3-3-1 symmetry at CLIC. *Eur. Phys. J. C*, v. 84, n. 2, p. 172, 2024.

[2] CHADWICK, J. Intensitätsverteilung im magnetischen Spectrum der β-Strahlen von radium B + C. *Verhandl. Dtsc. Phys. Ges.*, v. 16, p. 383, 1914. Disponível em: <http://cds.cern.ch/record/262756>.

[3] PAULI, W. in Septième Conseil de Physique, Solvay (Gauthier–Villars, Paris). p. 324, 1934.

[4] FERMI, E. An attempt of a theory of beta radiation. 1. *Z. Phys.*, v. 88, p. 161–177, 1934.

[5] SCHWINGER, J. S. A Theory of the Fundamental Interactions. *Annals Phys.*, v. 2, p. 407–434, 1957.

[6] BLUDMAN, S. On the universal fermi interaction. *Nuovo Cim 9*, p. 433–445, 1958.

[7] GLASHOW, S. L. Partial-symmetries of weak interactions. *Nuclear physics*, Elsevier, v. 22, n. 4, p. 579–588, 1961.

[8] WEINBERG, S. A model of leptons. *Phys. Rev. Lett.*, American Physical Society, v. 19, p. 1264–1266, Nov 1967. Disponível em: <https://link.aps.org/doi/10.1103/PhysRevLett.19.1264>.

[9] SALAM, A. in "elementary particle theory". *The Nobel Symposium no 8, edited by N. Svartholm (Almqvist and Wiksell, Stockholm)*, p. p. 367, 1968.

[10] NOETHER, E. Invariant variation problems. *Transport Theory and Statistical Physics*, Informa UK Limited, v. 1, n. 3, p. 186–207, jan. 1971. ISSN 1532-2424. Disponível em: <http://dx.doi.org/10.1080/00411457108231446>.

[11] WIGNER, E. *Group theory: and its application to the quantum mechanics of atomic spectra*. [S.l.]: Elsevier, 1959. v. 5.

[12] YANG, C. N.; MILLS, R. L. Conservation of isotopic spin and isotopic gauge invariance. *Phys. Rev.*, American Physical Society, v. 96, p. 191–195, Oct 1954. Disponível em: <https://link.aps.org/doi/10.1103/PhysRev.96.191>.

[13] QUIGG, C. *Gauge Theories of the Strong, Weak, and Electromagnetic Interactions: Second Edition*. USA: Princeton University Press, 2013. ISBN 978-0-691-13548-9, 978-1-4008-4822-5.

[14] NOVAES, S. F. *Standard Model: An Introduction*. 2000.

[15] BAGGOTT, J. E. *The quantum story: A history in 40 moments*. [S.l.]: Oxford University Press, USA, 2011.

[16] GOLDSTONE, J. Field Theories with Superconductor Solutions. *Nuovo Cim.*, v. 19, p. 154–164, 1961.

[17] ELLIS, J.; GAILLARD, M. K.; NANOPOULOS, D. V. A historical profile of the higgs boson. In: ____. *The Standard Theory of Particle Physics*. WORLD SCIENTIFIC, 2016. p. 255–274. Disponível em: <http://dx.doi.org/10.1142/9789814733519_0014>.

[18] JESUS Álvaro Santos de. Fenomenologia do mecanismo seesaw tipo-i. In: ____. [s.n.], 2020. Disponível em: <https://repositorio.ufrn.br/handle/123456789/29972>.

[19] BURDMAN, G. Lecture 20 - spontaneous breaking of non abelian gauge symmetries. In: ____. [s.n.], 2023. Disponível em: <https://fma.if.usp.br/%7Eburdman/QFT2/qft2index.html>.

[20] ABAZOV, V. M. et al. Measurement of the forward-backward charge asymmetry and extraction of $sin^2\theta_W^{\text{eff}}$ in $p\overline{p} \rightarrow z/\gamma^* + x \rightarrow e^+e^- + x$ events produced at $\sqrt{s} = 1.96$ TeV. *Phys. Rev. Lett.*, American Physical Society, v. 101, p. 191801, Nov 2008. Disponível em: <https://link.aps.org/doi/10.1103/PhysRevLett.101.191801>.

[21] WORKMAN, R. L. et al. Review of Particle Physics. *PTEP*, v. 2022, p. 083C01, 2022.

[22] THOMSON, M. *Modern particle physics*. [S.l.]: Cambridge University Press, 2013.

[23] AAD, G. et al. Observation of a new particle in the search for the Standard Model Higgs boson with the ATLAS detector at the LHC. *Phys. Lett. B*, v. 716, p. 1–29, 2012.

[24] PICH, A. *The Standard Model of Electroweak Interactions*. 2012.

[25] FUKUDA, Y. et al. Evidence for oscillation of atmospheric neutrinos. *Phys. Rev. Lett.*, v. 81, p. 1562–1567, 1998.

[26] AHMAD, Q. R. et al. Direct evidence for neutrino flavor transformation from neutral current interactions in the Sudbury Neutrino Observatory. *Phys. Rev. Lett.*, v. 89, p. 011301, 2002.

[27] CABIBBO, N. Unitary symmetry and leptonic decays. *Phys. Rev. Lett.*, American Physical Society, v. 10, p. 531–533, Jun 1963. Disponível em: <https://link.aps.org/doi/10.1103/PhysRevLett.10.531>.

[28] NIAMH O'C at English Wikipedia. 2013. Disponível em: <https://commons.wikimedia.org/w/index.php?curid=36881396>.

[29] HASERT, F. J. et al. Search for Elastic ν_μ Electron Scattering. *Phys. Lett. B*, v. 46, p. 121–124, 1973.

[30] ARNISON, G. et al. Experimental Observation of Isolated Large Transverse Energy Electrons with Associated Missing Energy at $\sqrt{s} = 540$ GeV. *Phys. Lett. B*, v. 122, p. 103–116, 1983.

[31] ARNISON, G. et al. Experimental Observation of Lepton Pairs of Invariant Mass Around 95-GeV/c**2 at the CERN SPS Collider. *Phys. Lett. B*, v. 126, p. 398–410, 1983.

[32] CERN. *Advancing the frontiers of technology*. 2024. Disponível em: <https://home.cern/about/what-we-do/our-impact>.

[33] PESKIN, M. E.; SCHROEDER, D. V. *An Introduction to Quantum Field Theory*. Reading, MA: Addison-Wesley, 1995. ISBN 978-0201503975.

[34] HAN, T. Collider phenomenology: Basic knowledge and techniques. *TASI*, 2005. Lectures given at Theoretical Advanced Study Institute in Elementary Particle Physics (TASI), Boulder, Colorado, USA, June 6-July 1, 2005. Disponível em: <https://arxiv.org/abs/hep-ph/0508097>.

[35] Wikipedia contributors. *Mandelstam variables — Wikipedia, The Free Encyclopedia*. 2024. https://en.wikipedia.org/wiki/Mandelstam_variables. [Online; accessed 31-July-2024].

[36] SCHWARTZ, M. D. Tasi lectures on collider physics. *arXiv preprint arXiv:1709.04533*, 2017. Disponível em: <https://arxiv.org/abs/1709.04533>.

[37] BUCKLEY, A.; WHITE, C.; WHITE, M. *Practical Collider Physics*. [S.l.]: IOP Publishing, 2021.

[38] FRANCESCHINI, R. et al. *Kinematic Variables and Feature Engineering for Particle Phenomenology*. 2022. Disponível em: <https://arxiv.org/abs/2206.13431>.

[39] ATLAS Collaboration. *13.6 TeV collisions 2024 - ATLAS Public Event Displays*. 2024. https://twiki.cern.ch/twiki/bin/view/AtlasPublic/EventDisplayRun3Collisions#13_6_TeV_collisions_2024. [Online; accessed 31-August-2024].

[40] ANGEL, S. L. C. *Standard Model of Electroweak Interactions*. 2024. Disponível em: <https://repositorio.ufrn.br/handle/123456789/57190>.

[41] BRUNNER, O. et al. *The CLIC project*. 2022. Disponível em: <https://arxiv.org/abs/2203.09186>.

[42] GURTU, A. Recent results from lep. *Pramana*, Springer, v. 54, p. 455–470, 2000.

[43] KAWAMOTO, T. LEP precision results. In: *LEP Symposium 2001: Beyond the Electroweak Scale*. [S.l.: s.n.], 2001.

[44] SADHUKHAN, S.; SINGH, M. P. Neutrino floor in leptophilic $U(1)$ models: Modification in $U(1)_{L_\mu - L_\tau}$. *Phys. Rev. D*, v. 103, n. 1, p. 015015, 2021.

[45] ANCHORDOQUI, L. A. et al. Leptophilic u(1) massive vector bosons from large extra dimensions. *Physics Letters B*, Elsevier BV, v. 820, p. 136585, set. 2021. ISSN 0370-2693. Disponível em: <http://dx.doi.org/10.1016/j.physletb.2021.136585>.

[46] MOROI, T.; NIKI, A. Leptophilic gauge bosons at lepton beam dump experiments. *Journal of High Energy Physics*, Springer Science and Business Media LLC, v. 2023, n. 5, maio 2023. ISSN 1029-8479. Disponível em: <http://dx.doi.org/10.1007/JHEP05(2023)016>.

[47] CHUN, E. J.; MONDAL, T. Leptophilic bosons and muon g-2 at lepton colliders. *JHEP*, v. 07, p. 044, 2021.

[48] LI, J. et al. A Comparative Study of Z$'$ mediated Charged Lepton Flavor Violation at future lepton colliders. *JHEP*, v. 03, p. 190, 2023.

[49] AGUILA, F. del et al. Collider limits on leptophilic interactions. *JHEP*, v. 03, p. 059, 2015.

[50] SPOR, S.; GURKANLI, E.; KÖKSAL, M. Search for the anomalous ZZγ and Z$\gamma\gamma$ couplings via $\nu\nu\gamma$ production at the CLIC. *Nucl. Phys. B*, v. 979, p. 115785, 2022.

[51] DASGUPTA, A. et al. Searching for heavy leptophilic Z': from lepton colliders to gravitational waves. *JHEP*, v. 12, p. 011, 2023.

[52] ALVES, A.; PROFUMO, S.; QUEIROZ, F. S. The dark $Z^{'}$ portal: direct, indirect and collider searches. *JHEP*, v. 04, p. 063, 2014.

[53] ALVES, A. et al. Dark Matter Complementarity and the Z$'$ Portal. *Phys. Rev. D*, v. 92, n. 8, p. 083004, 2015.

[54] ALVES, A. et al. Dirac-fermionic dark matter in U(1)$_X$ models. *JHEP*, v. 10, p. 076, 2015.

[55] ARCADI, G. et al. Dark sequential Z' portal: Collider and direct detection experiments. *Phys. Rev. D*, v. 97, n. 4, p. 043009, 2018.

[56] ALVAREZ, E.; ESTÉVEZ, M.; SEOANE, R. M. S. Z'-explorer: A simple tool to probe Z' models against LHC data. *Comput. Phys. Commun.*, v. 269, p. 108144, 2021.

[57] OSLAND, P.; PANKOV, A. A.; SERENKOVA, I. A. Updated constraints on Z' and W' bosons decaying into bosonic and leptonic final states using the run 2 ATLAS data. *Phys. Rev. D*, v. 103, n. 5, p. 053009, 2021.

[58] GHORBANI, K.; GHORBANI, P. H. DAMPE electron-positron excess in leptophilic Z' model. *JHEP*, v. 05, p. 125, 2018.

[59] KUNDU, S. et al. EFT analysis of leptophilic dark matter at future electron-positron colliders in the mono-photon and mono-Z channels. *Phys. Rev. D*, v. 107, n. 1, p. 015003, 2023.

[60] BURAS, A. J. et al. Global analysis of leptophilic Z' bosons. *JHEP*, v. 06, p. 068, 2021.

[61] YUE, C.-X. et al. Searching for the light leptophilic gauge boson Z $_x$via four-lepton final states at the CEPC*. *Chin. Phys. C*, v. 48, n. 4, p. 043103, 2024.

[62] AICHELER, M. et al. *A Multi-TeV Linear Collider Based on CLIC Technology: CLIC Conceptual Design Report*. Geneva: CERN, 2012. (CERN Yellow Reports: Monographs). Disponível em: <https://cds.cern.ch/record/1500095>.

[63] ROBSON, A.; ROLOFF, P. Updated CLIC luminosity staging baseline and Higgs coupling prospects. 12 2018.

[64] FRANCESCHINI, R. Beyond the Standard Model physics at CLIC. *Int. J. Mod. Phys. A*, v. 35, n. 15n16, p. 2041015, 2020.

[65] BLAS, J. de et al. The CLIC Potential for New Physics. v. 3/2018, 12 2018.

[66] SICKING, E.; STRÖM, R. From precision physics to the energy frontier with the Compact Linear Collider. *Nature Phys.*, v. 16, n. 4, p. 386–392, 2020.

[67] FeynRules Collaboration. *FeynRules: A Mathematica Package for Deriving Feynman Rules in Gauge Theories*. 2024. [Online; accessed 1-September-2024]. Disponível em: <https://feynrules.irmp.ucl.ac.be/>.

[68] ALWALL, J. et al. The automated computation of tree-level and next-to-leading order differential cross sections, and their matching to parton shower simulations. *JHEP*, v. 07, p. 079, 2014.

[69] SJOSTRAND, T.; MRENNA, S.; SKANDS, P. Z. A Brief Introduction to PYTHIA 8.1. *Comput. Phys. Commun.*, v. 178, p. 852–867, 2008.

[70] FAVEREAU, J. de et al. DELPHES 3, A modular framework for fast simulation of a generic collider experiment. *JHEP*, v. 02, p. 057, 2014.

APPENDIX A – Chapter 1

A.1 Pauli matrices

- **Definition**

Pauli matrices are complex unitary matrices

$$\sigma_1 \equiv \begin{pmatrix} 0 & 1 \\ 1 & 0 \end{pmatrix}, \sigma_2 \equiv \begin{pmatrix} 0 & -i \\ i & 0 \end{pmatrix}, \sigma_3 \equiv \begin{pmatrix} 1 & 0 \\ 0 & -1 \end{pmatrix}, \tag{A.1}$$

which are related to the $SU(2)$ group generators via $T_a = \sigma_a/2$, $a = 1, 2, 3$. Throughout this work we use the notation τ^a for Pauli matrices, but it is equivalent to the more conventional notation σ_a.

- **Commutation relation**

$$\left[\sigma_a, \sigma_b\right] = 2i\epsilon_{abc}\sigma_c \tag{A.2}$$

where

$$\epsilon_{abc} = \epsilon^{abc} = \begin{cases} 1, & \text{for even permutations of } abc \\ -1, & \text{for odd permutations of } abc \\ 0, & \text{otherwise.} \end{cases} \tag{A.3}$$

- **Hermiticity, determinant, and trace**

$$(\sigma_a)^\dagger = \sigma_a a, \quad \det \sigma_a = -1, \quad \mathrm{Tr}\, \sigma_a = 0, \tag{A.4}$$

Moreover,

$$\sigma_a^2 = \begin{pmatrix} 1 & 0 \\ 0 & 1 \end{pmatrix} = I. \tag{A.5}$$

A.2 Dirac gamma matrices

- **Dirac representation**

In terms of the *standard* or Dirac presentation, the Dirac matrices can be written as 4×4 matrices,

$$\gamma^0 = \begin{pmatrix} 1 & 0 & 0 & 0 \\ 0 & 1 & 0 & 0 \\ 0 & 0 & -1 & 0 \\ 0 & 0 & 0 & -1 \end{pmatrix}, \gamma^1 = \begin{pmatrix} 0 & 0 & 0 & 1 \\ 0 & 0 & 1 & 0 \\ 0 & -1 & 0 & 0 \\ -1 & 0 & 0 & 0 \end{pmatrix}, \gamma^2 = \begin{pmatrix} 0 & 0 & 0 & -i \\ 0 & 0 & i & 0 \\ 0 & i & 0 & 0 \\ -i & 0 & 0 & 0 \end{pmatrix},$$
$$\gamma^3 = \begin{pmatrix} 0 & 0 & 1 & 0 \\ 0 & 0 & 0 & -1 \\ -1 & 0 & 0 & 0 \\ 0 & 1 & 0 & 0 \end{pmatrix}. \tag{A.6}$$

The fifth Dirac matrix is given by

$$\gamma^5 = i\gamma^0\gamma^1\gamma^2\gamma^3 = \begin{pmatrix} 0 & 0 & 1 & 0 \\ 0 & 0 & 0 & -1 \\ -1 & 0 & 0 & 0 \\ 0 & 1 & 0 & 0 \end{pmatrix}, \tag{A.7}$$

or in terms of the Pauli matrices,

$$\gamma^j = \begin{pmatrix} 0 & \sigma_j \\ -\sigma_j & 0 \end{pmatrix}, \quad \text{with} \quad j = 1,2,3. \tag{A.8}$$

The γ^0 and γ^5,

$$\gamma^0 = \begin{pmatrix} I & 0 \\ 0 & -I \end{pmatrix}, \gamma^5 = \begin{pmatrix} 0 & I \\ I & 0 \end{pmatrix}, \tag{A.9}$$

- **Weyl (*chiral*) representation**

In this representation, the γ^5 is block-diagonal,

$$\gamma^0 = \begin{pmatrix} 0 & I \\ I & 0 \end{pmatrix}, \gamma^j = \begin{pmatrix} 0 & \sigma_j \\ -\sigma_j & 0 \end{pmatrix}, \gamma^5 = \begin{pmatrix} -I & 0 \\ 0 & I \end{pmatrix}. \tag{A.10}$$

Using this representation in the helicity projectors,

$$P_L = \frac{1}{2}(1-\gamma^5) = \begin{pmatrix} I & 0 \\ 0 & 0 \end{pmatrix}, \quad P_R = \frac{1}{2}(1+\gamma^5) = \begin{pmatrix} 0 & 0 \\ 0 & I \end{pmatrix}. \tag{A.11}$$

Applying in the chiral representation of a fermion $\psi = \begin{pmatrix} \psi_L & \psi_R \end{pmatrix}^T$,

$$P_L\psi = \frac{1}{2}\begin{pmatrix} I & 0 \\ 0 & 0 \end{pmatrix}\begin{pmatrix} \psi_L \\ \psi_R \end{pmatrix} = \psi_L, \tag{A.12}$$

$$P_R\psi = \frac{1}{2}\begin{pmatrix} 0 & 0 \\ 0 & I \end{pmatrix}\begin{pmatrix} \psi_L \\ \psi_R \end{pmatrix} = \psi_R. \tag{A.13}$$

- **Anticommutation and other relations**

Regardless the representation, the Dirac matrices must satisfy the anticommutation relation

$$\{\gamma^\mu, \gamma^\nu\} = \gamma^\mu\gamma^\nu + \gamma^\nu\gamma^\mu = 2g^{\mu\nu}, \tag{A.14}$$

since it obeys the Clifford algebra. The signs in the representations can change according to the signature of the metric $g^{\mu\nu}$. Other relations that all representations satisfy are

$$\gamma^{\mu\,\dagger} = \gamma^0\gamma^\mu\gamma^0 \tag{A.15}$$

$$\gamma^{5\,\dagger} = \gamma^5 \tag{A.16}$$

$$(\gamma^5)^2 = 1 \tag{A.17}$$

$$\{\gamma^5, \gamma^\mu\} = 0. \tag{A.18}$$

- **Some standard terminologies**

$$\text{scalar}: \quad I, \tag{A.19}$$

$$\text{vector}: \quad \gamma^\mu, \tag{A.20}$$

$$\text{tensor}: \quad \sigma^{\mu\nu} = \frac{i}{2}[\gamma^\mu, \gamma^\nu], \tag{A.21}$$

$$\text{pseudo-vector}: \quad \gamma^\mu\gamma^5, \tag{A.22}$$

$$\text{pseudo-scalar}: \quad \gamma^5. \tag{A.23}$$

The pseudo-vector and pseudo-scalar transform as a vector and a scalar, respectively, under continuous Lorentz transformations, but with an additional sign change under parity transformations.

A.3 Chirality operators

As discussed throughout this work, the chirality operators L and R when applied to a fermion ψ return the left-handed and right-handed chirality components respectively:

$$L \equiv \frac{1}{2}(1-\gamma^5) \quad ; \quad R \equiv \frac{1}{2}(1+\gamma^5). \tag{A.24}$$

In addition, we have relationships between the operators:

$$L + R = 1, \tag{A.25}$$
$$LR = RL = 0, \tag{A.26}$$
$$L^2 = L, \tag{A.27}$$
$$R^2 = R, \tag{A.28}$$

and knowing that $\bar{\psi} = \gamma^0 \psi^\dagger$, the Dirac adjoint of the chirality components of a fermion are given by:

$$\bar{\psi}_L = \bar{\psi} R = \bar{\psi} \left(\frac{1 + \gamma^5}{2} \right) \quad ; \quad \bar{\psi}_R = \bar{\psi} L = \bar{\psi} \left(\frac{1 - \gamma^5}{2} \right). \tag{A.29}$$

APPENDIX B – Chapter 2

B.1 Relativistic Fermi's golden rule

The Fermi's golden rule provides a way to calculate the transition rate from an initial quantum state i to a final quantum state f due to a perturbation. In non-relativistic quantum mechanics it can be written as

$$\Gamma_{if} = 2\pi \int |T_{if}|^2 \delta(E_f - E_i) dn, \tag{B.1}$$

where dn is the number of accessible states in the energy interval $E \to E + dE$, and T_{if} is the transition matrix element. For the process $a + b \to 1 + 2$, we can write the non-relativistic expression for the phase space as

$$dn = (2\pi)^3 \delta^3(\mathbf{p}_a + \mathbf{p}_b - \mathbf{p}_1 - \mathbf{p}_2) \frac{d^3\mathbf{p}_1}{(2\pi)^3} \frac{d^3\mathbf{p}_2}{(2\pi)^3}, \tag{B.2}$$

where $\mathbf{p}_i$ are the respective momenta of the particles. Furthermore, we can write the Lorentz-invariant matrix element $\mathcal{M}_{if}$ in terms of the transition matrix element of Fermi's golden rule, with the result that

$$\mathcal{M}_{if} = (2E_a \cdot 2E_b \cdot 2E_1 \cdot 2E_2)^{1/2} T_{if}. \tag{B.3}$$

Therefore, it is possible to write the Lorentz invariant version of Fermi's golden rule for the process $a + b \to 1 + 2$ as being

$$\Gamma_{if} = \frac{(2\pi)^4}{2E_a 2E_b} \int |\mathcal{M}_{if}|^2 \delta(E_a + E_b - E_1 - E_2) \delta^3(\mathbf{p}_a + \mathbf{p}_b - \mathbf{p}_1 - \mathbf{p}_2) \frac{d^3\mathbf{p}_1}{(2\pi)^3 2E_1} \frac{d^3\mathbf{p}_2}{(2\pi)^3 2E_2}. \tag{B.4}$$

B.2 Lorentz-invariant particle flux

For a process $a + b \to 1 + 2$, in which particles of type a and b have collinear velocities $\mathbf{v}_a$ and $\mathbf{v}_b$, as well as volumetric number density n_a and n_b, in a reference frame in which the particles b are stationary it is possible to write the incident flux of particles a as being:

$$\phi_a = (v_a + v_b) n_a. \tag{B.5}$$

When calculating the crosssection of this process, a term F known as **Lorentz-invariant flux factor** appears in the denominator , which is given by

$$F = 4E_a E_b (v_a + v_b). \tag{B.6}$$

If the moments and energies of the particles are respectively p_i and E_i, using the relation $v_i = p_i / E_i$, we can write F so that its Lorentz invariance is made explicit:

$$F = 4E_a E_b \left(\frac{p_a}{E_a} + \frac{p_b}{E_b} \right) = 4(p_a E_b + p_b E_a)$$

therefore,

$$F^2 = 16(p_a^2 E_b^2 + p_b^2 E_a^2 + 2E_a E_b p_a p_b).$$

To rewrite the third term of the previous equation, we will expand $(p_a \cdot p_b)^2$ considering that the velocities $\mathbf{v}_a$ and $\mathbf{v}_b$ are collinear:

$$\begin{aligned} (p_a \cdot p_b)^2 &= (E_a E_b + p_a p_b)^2 \\ &= E_a^2 E_b^2 + p_a^2 p_b^2 + 2E_a E_b p_a p_b \end{aligned}$$

After a series of simplifications we find the Lorentz-invariant flux factor in the form

$$F = 4[(p_a \cdot p_b)^2 - m_a^2 m_b^2]^{1/2}. \tag{B.7}$$

This form makes Lorentz invariance explicit since F is a function of Lorentz invariant quantities.

B.3 The Dirac delta-function

The Dirac delta-function $\delta(x)$ is a distribution in the form of an infinitesimally thin peak with unit area, it is defined as

$$\int_{-\infty}^{+\infty} \delta(x) dx = 1. \tag{B.8}$$

- **Other relations and properties**

For the distribution centered on $x = a$ and considering a function $f(x)$, we have the relation

$$\int_{-\infty}^{+\infty} f(x)\delta(x-a) dx = f(a). \tag{B.9}$$

Considering a non-zero scalar α, the delta-function satisfies the following scaling property

$$\int_{-\infty}^{+\infty} \delta(\alpha x)dx = \int_{-\infty}^{+\infty} \delta(u)\frac{du}{|\alpha|} = \frac{1}{|\alpha|}. \tag{B.10}$$

In the context of calculating the crosssection in equation (2.8), a useful relationship involving the Dirac delta function is the following

$$\int |M_{fi}|^2 g(p_1)\delta(f(p1))dp_1 = |M_{fi}|^2 g(p^*)\left|\frac{df}{dp_1}\right|^{-1}_{p_f^*} \tag{B.11}$$

where $f(p_1) = \sqrt{s} - \sqrt{m_1^2 + p_1^2} - \sqrt{m_2^2 + p_1^2}$, and $g(p_1) = \dfrac{p_1^2}{4E_1E_2}$. So that the result is $\dfrac{p_f^*}{4\sqrt{s}}|M_{fi}|^2$.

- **Conservation laws**

One of the possible uses of the Dirac delta-function is to impose conservation laws in integrals. The energy conservation of a decay $a \to 1+1$ for example is given by

$$\int_{-\infty}^{+\infty} ... \, \delta(E_a - E_1 - E_2)dE_1 \quad \Rightarrow \quad E_a = E_1 + E_2. \tag{B.12}$$

The momentum conservation for the same process is similar

$$\int_{-\infty}^{+\infty} ... \, \delta^3(\mathbf{p}_a - \mathbf{p}_1 - \mathbf{p}_2)d^3\mathbf{p}_1 \quad \Rightarrow \quad \mathbf{p}_a = \mathbf{p}_1 + \mathbf{p}_2. \tag{B.13}$$